The discrete porcine colonic lymphoglandular complex: Distribution and morphological features

by

David C. Morfitt

A Thesis Submitted to the
Graduate Faculty in Partial Fulfillment of the
Requirements for the Degree of
MASTER OF SCIENCE

Major: Veterinary Pathology

Iowa State University
Ames, Iowa

1986

TABLE OF CONTENTS

INTRODUCTION

The various epithelia and their adnexa enclose and protect the coelomic interior of higher animals, providing opportunity for maintenance of a controlled inner environment. Infectious disease, by definition, implies that one of these barriers, and frequently the enclosed body as well, are invaded, traversed, and disrupted by pathogenic agents. Secondary defenses are called to action in an attempt to reestablish normalcy.

This defensive response is most effective if prior sensitization to pathogens has been accomplished. At the same time, monitoring and recognition (tolerance) of "expected" or invited foreign material (e.g., foodstuffs) is necessary to avoid inappropriate responses (i.e., hypersensitization).

The gastrointestinal tract represents an expansive epithelial surface of the body and probably encounters more antigenic stimuli, in number, frequency, and concentration, than does any other. This suggests that it is the front at highest risk and that greater numbers of pathogenic organisms might select (or be selected for) this surface. However, the gastrointestinal tract is therefore also the site of greatest potential for controlled sampling of environmental antigens and subsequent immunization.

This study describes a lymphoepithelial organ of the porcine colon, the submucosal lymphoglandular complex (LGC). Distribution throughout the colon, with its large microbial and food antigen load, and a structure compatible with antigen sampling and transport capacity,

suggest a significant role for the LGC in maintenance of immune equilibrium.

LITERATURE REVIEW

In recent years, a great deal of research has been focused on the immunology of mucosal surfaces, including mechanisms of induction or delivery of responses (both cellular and humoral), secretory IgA, and interactions and interdependency of one site with another. Studies have shown that epithelia of the gastrointestinal, upper and lower respiratory, oral and salivary, genitourinary, mammary, and conjunctival and lacrimal mucosas are all potentially linked by immunoreactive cells, the lymphatics, and the circulatory system (37, 43, 47, 63).

The concept of a common mucosal immune system based on mucosa-associated lymphoid tissue (MALT) has arisen from these studies (6, 59). MALT, in turn, has been subdivided into four compartments based on location and morphology: 1) the scattered lymphoid cells of the lamina propria and interstitium; 2) intra-epithelial leukocytes; 3) scattered solitary or discrete "nodules" with organized lymphoid "follicles"; and 4) the aggregated follicular tissue found in the gut (the gut-associated lymphoid tissue, or GALT) and lung (the bronchus-associated lymphoid tissue, or BALT) (4, 5).

Also now well established is the concept of lymphoepithelium or follicle-associated epithelium (FAE) (9, 31), unique epithelial regions found in conjunction with both the discrete and aggregated lymphofollicular tissues of the digestive and respiratory systems (43). This epithelium is characteristically attenuated, consisting of a single layer of cuboidal or low columnar cells (9, 46, 60); contains few, if any, goblet cells (9, 46, 60); contains numerous, often clustered,

intra-epithelial leukocytes (generally lymphocytes) which cause it to appear disrupted (9, 46, 54); and contains specialized cells (M cells) (reviewed in 18, 68) responsible for facilitating contact of antigen with the immune system by selective, controlled, non-degradative (42) transport of macromolecules (9, 39, 42), fine particulate material (3, 9), viruses (14, 61, 70, 72), bacteria (47), chlamydia (32), and protozoans (36).

Cell populations present within lymphoepithelium seem to vary considerably between species. In the mouse Peyer's patch absorptive cells, goblet cells, M cells, tuft cells, and enteroendocrine cells are all present (11). Domes (63) in ileal Peyer's patches of gnotobiotic calves contain M-cells, columnar epithelial cells, and rare goblet cells (34). Cell types may also vary between organ systems in which they are located or between lymphoepithelial organs of distinct configuration (e.g., aggregate vs. solitary).

Common to all lymphoepithelia are facilitated approach of environmental antigen and controlled uptake and transport of it to underlying lymphoid cells and macrophages (43). These functions are achieved by a somewhat variable population of cells known collectively as FAE cells or M cells (for membranous cell) (9, 42).

M cells are characterized by morphological peculiarities. Though they share tight junctions with adjacent columnar epithelial cells, they are distinguished from them by short, irregularly oriented, sometimes wider, and sparse microvilli; microvillous rootlets and apical terminal webs which are both poorly defined; cytoplasmic organelles such as

mitochondria present in the apical zone; abundant numbers of apically oriented vesicles and tubules; scarce lysosomes; basally positioned nuclei which are often indented and folded; and lastly, by intraepithelial lymphocytes or macrophages, frequently clustered together and enclosed within indentations or hollows of the cell (13; 31, 42).

This thin cytoplasmic border, easily accessed by luminal material, separates the outer world and its insults from the lymphoid system reponsible for defending higher animals. GALT, in concert with other components of the MALT system, is now recognized as providing portals necessary for immune sensitization across its mucosal surfaces (43).

Authors have emphasized the tonsils, Peyer's patches, and appendix when discussing GALT, and only scant reference is made to structures located in the large intestine. This is despite many diseases being localized wholly or in part to the large intestine (e.g., swine dysentery due to Treponema hyodysenteriae, enteric salmonellosis, and hog cholera), and subsequent alteration of colonic lymphoid structures (2, 21, 22, 50, 66).

Submucosal extensions of colonic epithelium (glands, diverticula) are typically associated with nodular lymphoid tissue. They are reported, in either normal or pathologic form, in many species, including swine (Klein (1898), cited in 7; 7, 17, 21, 24, 27), cattle (24, 52), sheep (24), dogs (1, 24), cats (24), the Australian echidna (55), guinea pigs and horses (Retterer (1892), cited in 52), primates (Orth (1901), cited in 21), and man (30, 64).

Published work presents a confusing picture of intestinal submucosal glands. Distribution varies between species, and reports on the same species may disagree. In the dog, for example, they are described by some authors as being restricted to the cecum and immediately adjacent colon (1), while others indicate that they occur throughout the canine intestine (24). In the pig they occur throughout the intestine but are most prevalent in the ileum (24).

In swine, "solitary lymph nodules", present in the entire intestinal tract, are "...more concentrated in the distal parts of the tract" (40). This is in contrast to aggregated patches of lymph nodules which, although most common in the small intestine, are also found in small numbers trailing from the ileocecal valve into the ascending colon (40). Others treat the discrete "lymphoid follicle" as a structure unique to the porcine large intestine (27). Authors agree, though, that very few "nodules", "follicles", or "submucosal glands" are present in the cecum of the pig (24, 27, 40), with 84-89% reportedly present in the colon, and 11-16% in the rectum (27).

Total number of porcine colonic "submucosal glands" or "lymphoid follicles" varies widely between pigs (7, 27) and between regions of the colon (7). Between one and six weeks of age the total number increases from an average of 520 to 1149 (27). Number per 10 cm^2 of bowel wall increases slightly between one and three weeks (31.9 to 33.9) and then decreases to 17.2 by six weeks of age (27).

In addition to the inconsistent distributions reported (and perhaps as the basis for it), there is discrepancy in identification and

designation of submucosal glands and LGCs. Some authors include or cite descriptions of structures such as Brunner's glands (24) or epithelial penetration into aggregated lymphoid tissue such as Peyer's patches (19, 24, 55). Hebel separates three submucosal gland types on the basis of configuration: 1) Büschel (bush) glands 2) Strauch (branched) glands and 3) dilated or cystic glands (24). Elias describes two: 1) luminal diverticula and 2) submucosal chambers deriving from multiple colonic crypts (19). Others consider these differences normal (7, 52).

Hebel also defines three forms of epithelial penetration through the muscularis mucosae according to the appearance of the muscularis: 1) ends of the muscularis fold back on themselves where crypts pass through to the submucosa 2) thin and thick layers of muscularis abut abruptly against the outermost epithelial crypts 3) a reticulate muscularis with smooth muscle interweaving around and between separate crypts (24).

Though differences in color and tissue density distinguish LGCs from remaining intestinal wall (7), various techniques have been utilized to enhance LGC visibility for gross and low power microscopic study. Dukes and Bussey (16), using formalin-fixed human colons, removed as much of the muscular tunics as possible and scraped off the entire mucosal layer. Remaining tissue was stained in aqueous methylene blue (1-2%), rinsed in water, "differentiated" in "dilute" acetic acid, and spread between plates of glass for study. Inoue and Sugi, in their study of porcine small and large intestine (27), employed the same method used by Cornes for human small intestine (15). Intestine was opened and washed in running water, fixed in dilute acetic acid, stained

with 0.5% methylene blue, and rinsed. Lymphoid tissue was visualized by transillumination.

Colonic submucosal glands are considered normal in most species (see above). Others apply terms such as "microhernia" (56) and regard them instead as pathologic or dependent on pathological weakening of the muscularis mucosae (52).

Cystic, epithelially lined submucosal diverticula are the hallmark lesion of "colitis cystica profunda" of man (23). The presence of glandular epithelium in the submucosal region is regarded as abnormal, arising either by "herniation" through congenital or acquired "defects" in the muscularis mucosae, or from re-epithelialization of deep ulcers or abscesses (20). Similar lesions in the colons of animals (dog, cat, cattle, gibbon, mouse) are also considered "transgressions" of epithelium across the muscularis mucosae or "downgrowths" into submucosal lymph nodules (62). Of the domestic species, the condition is said to be "perhaps most often seen in swine" and is described as "dilated colonic glands protruding through the muscularis mucosae" which "may be a sequel to colitis and local damage to the muscularis mucosae, or it may represent herniation into the space left by an involuted submucosal follicle" (2).

Colonic LGCs of the dog consist of submucosal lymphoid nodules "invaginated" by glands which pass through a "deficiency" of the muscularis mucosae. The glandular epithelium is squamous to columnar with only a few goblet cells present. Apical secretory granules are less obvious in the submucosal columnar epithelial cells than in their

mucosal counterparts. Many intraepithelial lymphocytes are present (often nested), and no enterochromaffin cells are observed. Neither cortical-medullary division nor germinal centers are seen in the lymphoid nodules (1).

Intestinal "lymphoepithelial glands" of the Australian echidna (spiny anteater) are similar in form to the porcine colonic LGC (see below). Columnar, goblet, and enterochromaffin cells are reported "indistinguishable" from analogous mucosal cells. Paneth-like cells are also present. Intraepithelial lymphoid cells are prominent and sometimes clustered. Pale, less dense, "medullary" areas of the lymphoid nodules lie next to epithelial diverticula (55).

Corresponding structures in the human colon are designated "lymphoid-glandular complexes" or "microbursae" (30).

Though submucosal penetration by epithelial diverticula is not described in colonic lymphoid patches of the rat, lymphoid "follicles" occupy both mucosal and submucosal regions and the overlying epithelium is distinguished by intraepithelial lymphoid cell clusters, the absence of mature goblet cells, and the preferential binding and uptake of luminal particulate material (8).

Biswal et al. describe the submucosal gland of the porcine large intestine as a tubular, branched, glandular arrangement embedded in lymphoid tissue and communicating with the intestinal lumen "through" the muscularis mucosa. Lining epithelium reportedly consists of two cell types, columnar (resembling surface epithelium) and goblet cells (which are common) (7). Hebel asserts that goblet cells are fewer in

number relative to adjacent colonic epithelium (24).

Though normally visible grossly in all but very young pigs (7), the glands enlarge and become even more prominent in various disease states (21, 22, 66). As such, they are microscopically dilated, contain increased amounts of secretory products or necrotic debris, and show decreased PAS (periodic acid-Schiff) staining and size of goblet cells (21, 66). Specific diseases in which changes of this nature have been observed include swine dysentery (T. hyodysenteriae) (2), balantidiosis, porcine enteric salmonellosis, and campylobacterosis (J. F. Pohlenz, Dept. Vet. Pathology, Iowa State University, personal communication; author's observation).

Though one report concludes changes of this nature to be secondary to the diarrheal process (21), another speculates that the submucosal glands may be the foci of inflammatory changes in certain infections of the porcine colon and that "study of their precise pathology remains to be made" (7).

Over thirty years ago colonic submucosal gland function was considered "unknown" but "assumed identical to the mucosal (intestinal) glands" (7); a well defined answer is still not available and no thorough morphological study, particularly of ultrastructural features, could be found.

Realizing that effective pathological studies are based on firm understanding of normal form and function, the present study has been undertaken with these objectives:

1. To establish sound methods for identifying and evaluating discrete LGCs in the porcine large intestine.

2. To enumerate and investigate patterns of distribution of the LGCs.

3. To assess the consistency of lymphoepithelial association in colonic lymphoid nodules and its microscopic morphology.

4. To investigate the cellular composition of the epithelial component of the lymphoglandular complex (LGC).

MATERIALS AND METHODS

Materials

Animals utilized

Tissues studied were collected from fourteen conventional pigs maintained on a standard growing diet. The pigs comprised two litters of seven pigs each which were both obtained at three weeks of age, but which differed in age by 31 days. Upon arrival, the younger litter was mixed in with the older. Individual animals were not formally randomized, but rather simply picked by "ease of catching" when an animal of a given age was sacrificed. Aside from transient diarrhea and mild sneezing at the time of arrival, no clinical disease was observed and none of the animals showed any gross lesions at necropsy.

Drugs, reagents, formulations

Details on drugs, reagents, and formulations referred to in the text are listed in Appendix A.

Methods

Specimen collection

Tissues, used for either counting LGCs or evaluating microscopic morphology, were collected by two different methods.

For counting To identify and enumerate LGCs or simple lymphoid nodules a technique based on staining with methylene blue (MB) (15, 27) was adopted. Single animals, at approximately 5, 9, 10, 11, and 12 weeks of age, and two at 13 weeks of age were used (see Appendix B).

Animals were killed by electrocution. Large intestine (including cecum, ileocecal valve (ICV), colon, rectum, and anus) was removed immediately and the intestine dissected free of mesentery. Intestines were then opened longitudinally by incising along the antimesenteric border and fecal material was removed by gentle washing with cold tap water.

Opened and cleaned specimens were then placed into five gallon plastic pails and allowed to tumble in a cold running water bath for times ranging from 15 1/2 to 20 1/2 hours (see Table 1).

Once initial processing of the large intestine was completed, a gross post mortem examination of the pig was carried out.

After the cold water wash, specimens were transferred to pails containing 12 liters of dilute acetic acid (see Table 1) and left for periods of 18 1/2 to 32 1/4 hours.

After fixation in the acetic acid, specimens were stained briefly in a 0.5% MB solution and then rinsed in water to remove excessive background stain (see Table 1).

For microscopy Specimens for microscopic studies were collected from animals at approximately 4, 6, 10, 11 (two), and 12 (two) weeks of age (see appendix B).

Animals were anesthetized by intravenous (cranial vena cava) administration of sodium pentobarbital and placed in right lateral recumbency.

A large incision was made at the left flank and the spiral colon was exteriorized. Adjacent paired segments of descending, distal

(centripetal) spiral, and proximal (centrifugal) spiral colon were

Table 1. Processing Parameters for Gross Count

Pig age (weeks)	5	9	10	11	12	13(1)	13(2)
Wash time (hours)	20.5	16	15.75	17	17	15.5	15.5
Acetic acid fixation (hours)	32.25	24.3	18.5	23.5	25.0	21.0	21.0
-concentration	5%	2%	5%	3%	3%	5%	5%
-under refrigeration	+	-	+	-	-	-	-
Methylene blue staining (seconds)	60	60	60	60	90	75	75
Rinse (hours)	4.3	4.5	4.3	2.5	2.0	4.0	4.0

ligated and then infused until softly turgid with either 10% neutral buffered formalin (NBF) or a cold (4°C) solution of 3% glutaraldehyde and 0.1 M cacodylate buffer, pH 7.3. Once infused, the segments were severed from the adjoining colon, immersed in vials of like fixative, and stored under refrigeration.

Exceptions to this procedure included opening and immersion fixation of all specimens from the 4-week old pig and the NBF fixed specimens from the 6-week old pig; formol sublimate was substituted for NBF with one 12-week old pig.

With the 6-week and one 11-week old pigs, attempts were made to isolate, bisect, and reimmerse in fresh glutaraldehyde fixative several LGCs from each section soon after infusion and collection of the loops. The intent was to minimize post mortem degenerative changes by facilitating entry of glutaraldehyde to the submucosal regions.

Evaluation of count and distribution

Total and segmental counts and distribution patterns of LGCs were determined by viewing the MB-treated colons over transmitted light (see Figures 1 and 2). Colons were laid flat in a clear glass dish set atop a commercial fluorescent viewing box. Lengths and widths of consecutive segments of colon wall were recorded as well as the number of LGCs observed in each. An attempt was made to keep widths and LGC density (i.e., number per unit area of intestinal wall) uniform across a given segment.

Photographs of MB-stained colons were made utilizing a dissecting photomicroscope (Tessovar, Carl Zeiss, W. Germany) and Kodak Plus-X Pan with an orange #22 filter for black and white prints or Kodak Kodachrome 40-Type A 5070 unfiltered for color transparencies (Eastman Kodak, Rochester, NY).

Light microscopic studies

NBF fixed tissues from 4-, 10-, 11-, and 12-week old pigs were used for light microscopic studies.

Ligated loops collected after infusion fixation were opened, fecal material was rinsed away, and individual LGCs were identified and trimmed free.

Identity of LGCs was verified and any necessary additional trimming (e.g., bisection) of LGCs was performed under a dissecting microscope using transmitted light.

Paraffin blocks of individual formalin fixed specimens were prepared by dehydrating tissues through graded concentrations of ethanol

Figure 1. Segment of distal spiral colon from a 12-week old pig; tissue was fixed in acetic acid and stained with methylene blue. LGCs are visible by transmitted light as densities scattered randomly but evenly across the intestinal wall. Central pores are seen as clear spots in the centers of many, but not all. Note how tissue folds, shadows, and stain densities tend to hide the LGCs (see also Fig. 2). Bar=1cm

Figure 2. From same pig as tissue in Fig. 1. Segment from the proximal spiral colon just beyond the last of the aggregated masses associated with the ileocecal valve. LGCs are scarce in this area. In all pigs they were rare or absent between this level and the ileocecal valve. Bar=1cm

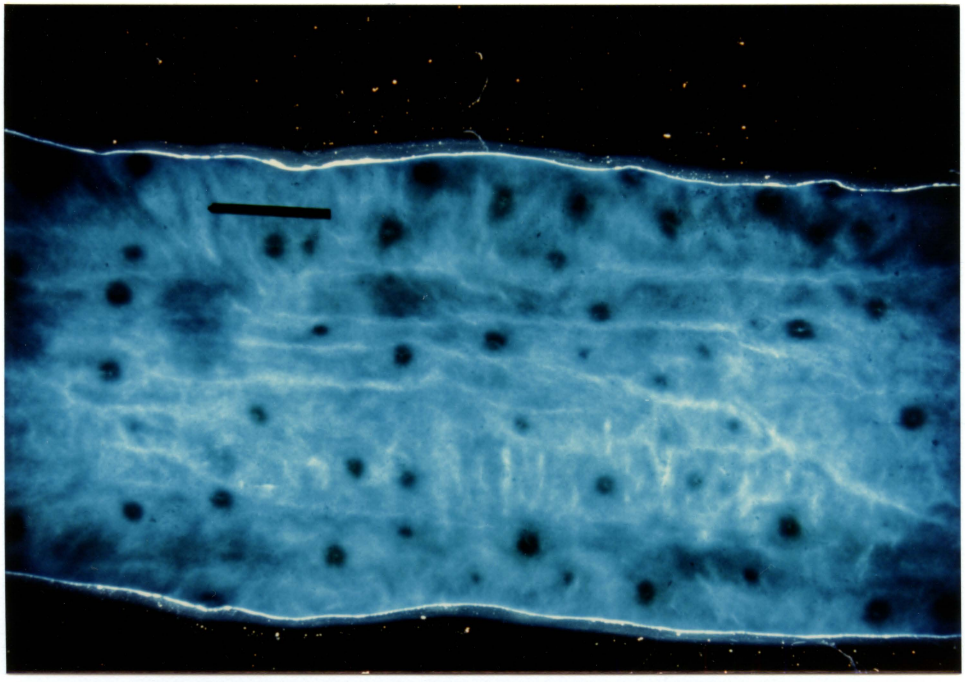

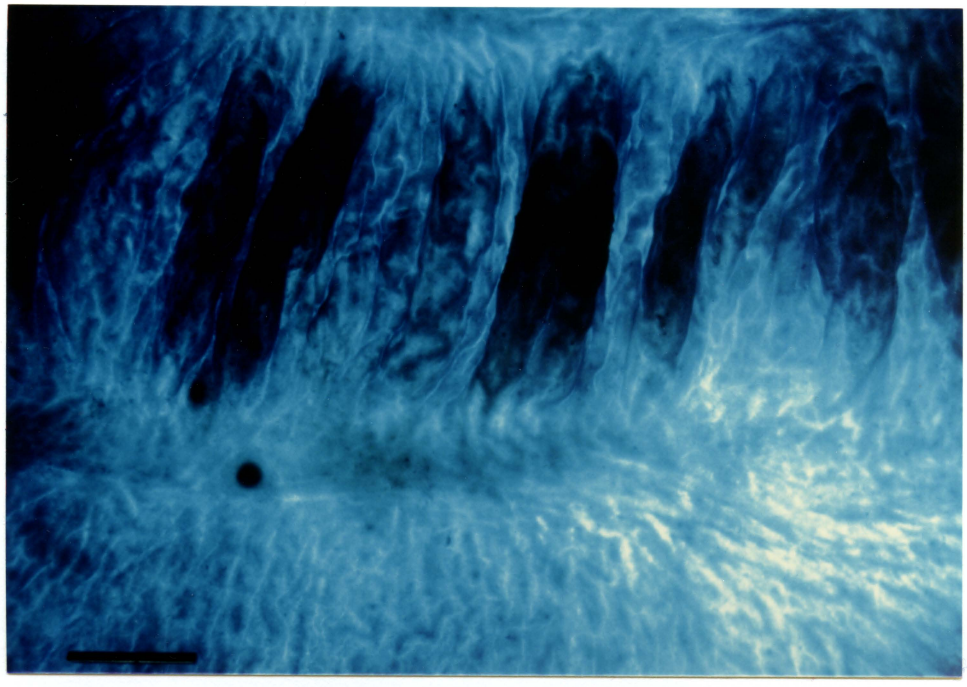

(70-100%), clearing in xylene, and infiltration and embedding with liquid paraffin. Five um sections were cut, floated on warm water, and picked up onto glass slides. Standard techniques were employed to stain tissues with Harris's hematoxylin and eosin (H&E) (48) or, in selected cases, with Gomori's one-step trichrome stain (57). Cover slips were mounted with Permount®.

Additional selected blocks were prepared by plastic embedding. Individual specimens (either NBF or glutaraldehyde fixed) were dehydrated through graded alcohols (50-100%) and infiltrated and embedded in infiltrating and embedding media (glycol methacrylate; JB-4®, Polysciences, Inc., Warrington PA). Blocks were allowed to harden under vacuum for at least fifteen hours.

Serial sections Individual LGCs contained within small squares of colon wall were utilized.

Paraffin embedded The outer muscular tunics were carefully dissected away after fixation to prevent curling of the specimens during processing and to allow them to be embedded flat or vertically erect within paraffin blocks. Orientation in these two different planes permitted sectioning both parallel with or perpendicular to the luminal surface of the gut wall.

Consecutive 5 um sections were made of the blocks, laid out and numbered in order, and stored. Sufficient numbers of sections were selected and stained to provide an accurate impression of overall LGC morphology.

Plastic embedded Blocks were prepared of specimens both with and without muscular tunics present; curling of specimens did not occur as in the paraffin technique.

Consecutive 3 um sections were cut on a JB-4 microtome (Porter-Blum, Newtown CT) using Ralph knives, floated on a distilled water bath, picked up onto acid alcohol cleaned slides, and dried for 10 minutes on a hot plate at 60-70°C. (One drop of NH_4OH per 100 ml distilled H_2O was added to the water bath to enhance spreading.) Sections were routinely stained in 1% toluidine blue (1-6 minutes), rinsed in distilled H_2O, and blow dried with hot air. Cover slips were mounted with Permount®.

A small series of slides were stained by a rapid H&E method by dipping them briefly in distilled water and staining for 15 minutes in Harris' hematoxylin (Surgipath®). Sections were then rinsed, differentiated in 1% acid alcohol, blued in lithium carbonate, stained for two minutes in alcoholic eosin-y (Shandon®), dehydrated in ethanol, cleared in xylene, and mounted in Permount®.

Evaluating uniformity of lymphoid nodule-gland association NBF infused tissue from an 11-week old pig was used. A 2 cm long, whole circumference segment was cut from each of the three infused loops available (proximal spiral colon, distal spiral colon, and descending colon). Segments were incised, laid flat, and scrutinized carefully using transmitted light as described above to detect discrete densities composed of one or more lymphoid nodules. The discrete specimens (35 total) were collected separately and bisected in a plane perpendicular to the mucosal surface.

Taking care to minimize tissue loss when first sectioning blocks, 5 um sections were cut, stained with H&E, and evaluated for consistency of morphological features.

Photomicrographs of histologic sections were taken using a Vanox Photomicroscope with a PM-10ADS automatic photomicrographic system (Olympus, Japan) and Kodak Panatomic-X print film (Eastman Kodak, Rochester NY).

Ultrastructural studies

Glutaraldehyde fixed tissues from 6-, 10-, 11- (two) and 12-week old pigs were utilized. Specimens were isolated as for light microscopy studies, but special care was taken to avoid drying of the outer surfaces.

Scanning electron microscopy LGCs within SEM specimens were left intact, vertically bisected (using razor blades and a dissecting microscope), or cut into four pieces by perpendicular cuts intersecting at the central pore. Fixed and trimmed specimens were washed with a stream of buffered fixative from a squirt bottle to remove surface debris and mucus.

A method involving tannic acid was used to process tissues as follows: 1) overnight immersion and mechanical rotation of tissues in vials containing 3 ml of GTA solution (3% glutaraldehyde and 8% tannic acid) at room temperature 2) two 15 minute rinses in 0.1M cacodylate buffer, pH 7.3 3) rotation for 30 minutes in a 0.5% osmium tetroxide, 0.1M cacodylate buffer, pH 7.3 solution 4) six rinses in distilled H_2O over 15 minutes 5) stirring for 1 hour in aqueous 5% tannic acid 6)

three rapid distilled H_2O rinses 7) stirring for 1 hour in aqueous 0.5% OsO_4 8) six rinses in distilled H_2O over 15 minutes 9) dehydration through 15 minutes each of 50, 75, 95, and 100% solutions of ethanol; 15 minutes each in 3:1, 1:1, and 1:3 ethanol:freon solutions; two 15 minute periods in 100% freon; all with rotation.

Specimens were then critical point dried from liquid CO_2 (DCP-1 Critical Point Drying Apparatus, Denton Vacuum, Inc.) and mounted using silver paint on stubs with either the central pore (mucosal surface) or cut edge of the complex facing upward. Specimens were sputter coated with gold and palladium (Edwards E306) and examined with a Cambridge Steroscan 200 scanning electron microscope.

Transmission electron microscopy Specimens were either bisected in a median plane through the central pore or a slab of complex was isolated by two parallel perimedian cuts on either side of the central pore.

Processing was carried out as follows: 1) fixation in fresh glutaraldehyde fixative for one hour 2) two 15 minute rinses in 0.1M cacodylate buffer, pH 7.3 3) post-fixation in 1% OsO_4 in 0.1M cacodylate, pH 7.3, for one hour 4) three brief rinses in distilled H_2O 5) dehydration through an acetone series using a mechanical rotator: 15 minutes each in 50, 75, and 95% acetone; two 15 minute periods in 100% acetone; two further 15 minute periods using 100% acetone from a fresh bottle.

Specimens were infiltrated with a 1:1 mixture of 100% acetone and epoxy resin for two hours, pure resin for eight hours, and then eight

more hours in a vial of fresh pure resin. Specimens were placed in a vacuum oven at 45°C and 56 cm Hg for 20 minutes to enhance infiltration and again after embedding in either gelatin capsules or flat molds. Blocks were cured overnight at 60°C.

Thick sections were cut at 3 um using glass knives (made with a KnifeMaker, LKB, Sweden) on an ultramicrotome (model 8800, LKB, Sweden) and stained for light microscopy on a hot plate at 90-95°C with an aqueous solution of 1% toluidine blue and 1% sodium borate. Areas were selected for thin sectioning and the blocks trimmed. Thin sections of 60-90 nm were cut using diamond knives on an ultramicrotome (model 4801, LKB, Sweden). Sections were mounted on 3 mm diameter copper grids, stained with uranyl acetate and lead citrate, and evaluated on a Hitachi HS-9 transmission electron microscope.

Pilot studies

Tissues from 10 animals unrelated to the above were used in a variety of preliminary trials. Sources for these pigs included three research projects (8 pigs) unrelated to the present and routine submissions (2 pigs) to the Iowa Veterinary Diagnostic Laboratory. Details on use are included in Appendix C.

RESULTS

Counts

Results of counts of LGCs visible by the methylene blue technique are given in Table 2.

Table 2. LGCs counted in colons of 6 pigs examined

Pig age (wk)	5	10	11	12	13	13		
Litter	Y	0	0	0	Y	Y		
							Means	
Total count	1068	1111	1408	1499	1256	1043	1231	
						Y	1122	NS[a]
						0	1339	

[a]NS: nonsignificant difference by Student's t, $p<0.1$

No significant difference exists between the mean counts for the two litters used (though pigs used were not randomized before selecting; see Materials and Methods).

Over a given segment of colon LGCs were evenly and randomly distributed (see Figure 1).

Discrete lymphoid aggregates seen in the cecum were counted, but not included in the totals for colons. Cecal counts ranged from 2 to 19; the mean was 10.

Results obtained from the 9-week old pig (see Appendix B) are not included in Table 2. In that instance, only LGCs with readily visible central pores were counted; 947 were identified.

A small fraction of LGCs (roughly one in forty) in colons from all

animals showed no central pore as viewed under the dissecting microscope.

Distribution

Density, or number of LGCs per unit area of bowel wall, varied by region and showed an age-associated trend.

The graphs presented in Figure 3 detail the number of LGCs present in the six colons counted using the central flexure of the spiral colon, "CF", as a common reference point.

Raw counts (summarized in Table 3) were converted to area densities (number/10 cm^2). The histograms indicate mean densities over given increments of linear length.

Very few or no LGCs were present in the proximal 7-12% of all colons examined (see Figure 2).

LGCs were concentrated somewhat toward the central regions with fewer present toward either end (this was least evident in the older animals). This same trend was evident from "regional means" calculated from the raw count figures (see Table 3).

Maximum densities ranged from a high of 45.4/10 cm^2 in the descending colon of the 5-week pig to 12.8/10 cm^2 fifty centimeters distal to the central flexure of one 13-week pig and 8.3/10 cm^2 in both the proximal and distal spiral colon of the other 13-week pig.

Area density of LGCs was lower and more uniform in the 13-week old pigs compared with the younger animals. Absolute counts of LGCs present from the central flexure distally ranged from 628 (13-week pig) to 962

Figure 3. Distribution of LGCs visualized by methylene blue staining in colons of six experimental pigs. Graphs indicate the area density over the entire extent of the colon from A, anus, to ICV, the ileocecal valve. CF, the central flexure of the spiral colon, is used as a common reference point (0) from which linear distances are indicated in 20 cm increments both cranially and caudally

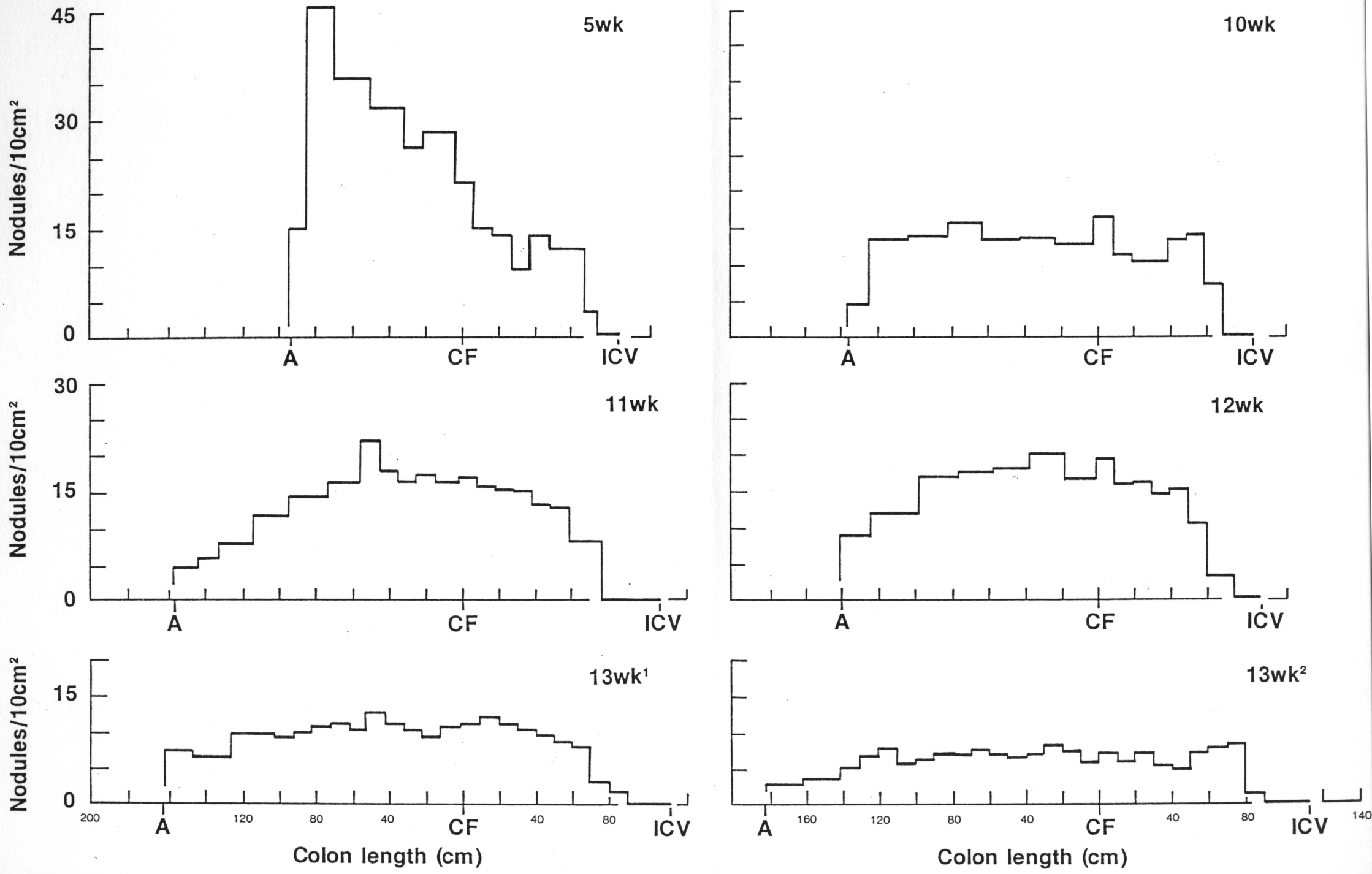
5wk
10wk
11wk
12wk
13wk¹
13wk²
Nodules/10cm²
45
30
15
0
A
CF
ICV
200
120
80
40
160
140
Colon length (cm)

(12-week pig) with a mean of 762 and standard deviation of 118 (see Table 3).

Table 3. Raw counts by region of colon

Pig age (wk) / Litter / Segment	5 Y	10 0	11 0	12 0	13 Y	13 Y	Means
rectum	41	34	48	100	83	52	60
descending colon	127	105	73	130	118	74	105
distal spiral colon — distal half	252	269	248	327	248	224	261
distal spiral colon — proximal half	279	287	447	405	320	278	336
central flexure	- - -	- - -	- - -	- - -	- - -	- - -	- - -
proximal spiral colon — distal half	223	256	459	400	365	259	327
proximal spiral colon — proximal half	146	160	133	137	122	156	142
cecum	19	2	6	13	14	5	10
TOTAL	1087	1113	1414	1512	1270	1048	1241

Microscopic Evaluations

Morphological uniformity

To assess the microscopic structural variability between the 35 specimens containing individual and aggregate lymphoid nodules, the following features were evaluated and recorded: the presence or absence of 1) submucosal epithelial diverticula; 2) a well defined gap in the muscularis mucosae; and 3) obvious germinal centers within lymphatic nodules. Results are shown in Table 4.

The specimens examined were highly uniform with respect to presence of submucosal diverticula, gaps in the muscularis mucosae, and germinal

centers.

Table 4. Uniformity between discrete lymphoid aggregates

	descending colon	distal spiral colon	proximal spiral colon
Number of discrete aggregates examined	8	19	8
Submucosal epithelial diverticula present	8	19	7[a]
Gaps visible in the muscularis mucosae	8	19	7[b]
Germinal center(s) in nodule(s)	8	19	8

[a] In the single exception, the entire lymphoid mass was sectioned away from the block containing one half of the specimen; though impossible to prove, it is suspected that the other half was also sectioned too deeply.

[b] In one instance, though presence of the gap was inferred from a downfolding of the muscularis mucosae, the actual gap was not observed.

Histologic morphology

Colonic LGCs consist of one or more well defined lymphatic nodules and interposed lymphoid cells situated within the submucosa (see Figures 4-6). Nodules contained pale staining, well defined germinal centers with numerous tingible body macrophages and, oriented toward the LGC center, coronas composed of small dark lymphocytes. Size and number of nodules (and therefore overall LGC dimensions) were highly variable, with 1 to 12 present; LGCs in the descending colon appeared generally larger.

Internodular lymphoid tissue was sometimes restricted to the

Figure 4. LGC from the proximal spiral colon of an 11-week old pig; NBF infused colon; paraffin embedded; H&E staining. Surface pore, epithelial diverticula passing through a gap in the muscularis mucosae, and a germinal center with its corona of small lymphocytes are all visible. A few leukocytes, both PMN and mononuclear, lie within a diverticular lumen. X 41

Figure 5. LGC from the same animal as Fig. 4; descending colon. In this less common form the perinodular lymphoid tissue of the complex infiltrates the mucosa where it separates and displaces mucosal glands. X 44

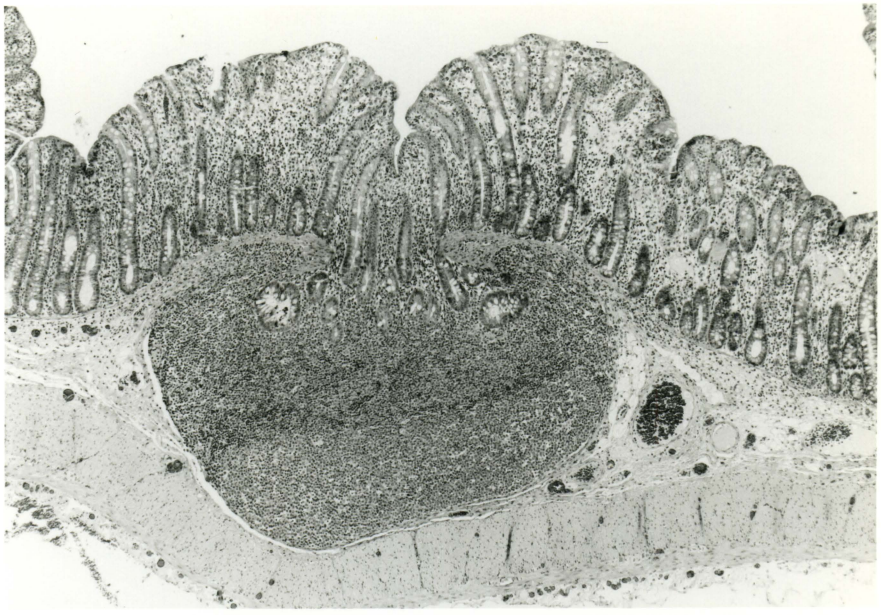

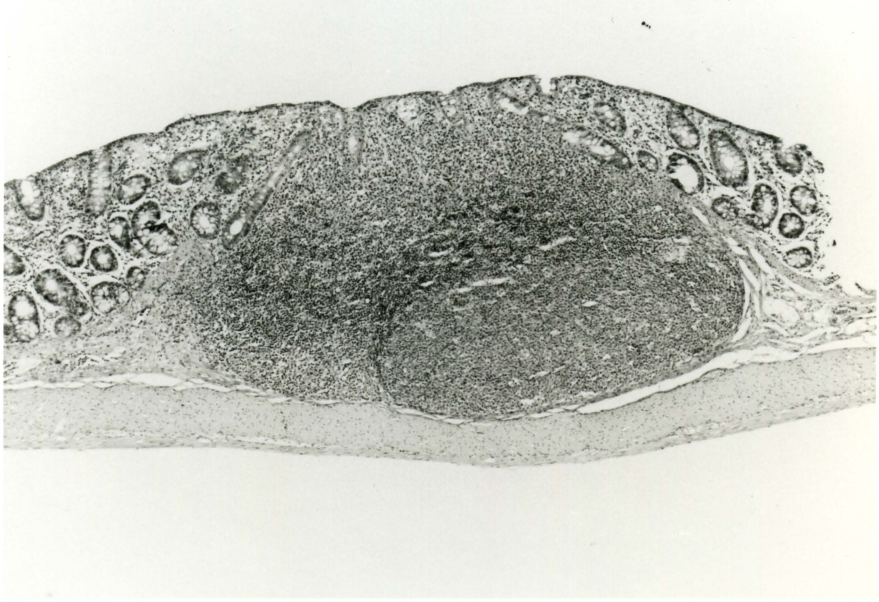

Figure 6. LGC from the descending colon of a 12-week old pig. a-d) Four sections selected from a serial set cut parallel to the surface of the colon. NBF fixation. Glycol methacrylate embedding. Toluidine blue staining. a) Deep in LGC. Eleven distinct lymphatic nodules with germinal centers are present. Clear spots within germinal centers represent tingible body macrophages. Only four diverticular outlines are present (upper left); most of the epithelial component lies above this level. b) Higher level. Radial pattern of the diverticula is prominent. Extremities of the diverticula are expanded and sac-like. The central pore shows diverticula emanating from it. A portion of the circular fold of muscularis mucosae (arrows) borders diverticula passing from the mucosa into the submucosa where they pass well beyond the collar. c) Higher level. d) Highest level. All submucosally located epithelium is left behind. The collar of muscularis mucosae is completed (arrow). X 22

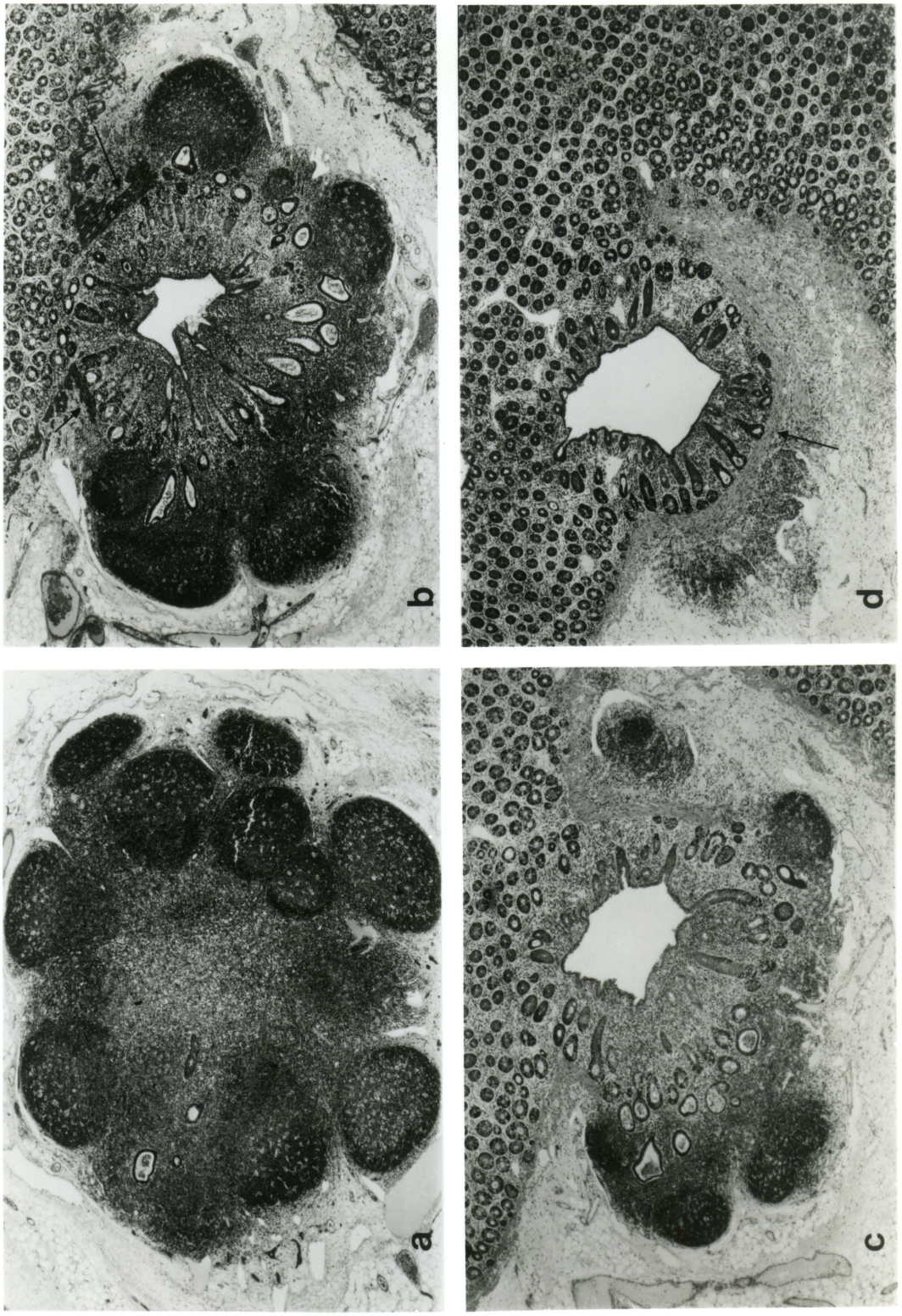
b
d
a
c

submucosa and sometimes extended upward into the mucosa where it might displace mucosal crypts (see Figure 5).

Pattern and configuration of epithelial penetration into the submucosal lymphoid tissue were, in sections cut perpendicularly to the luminal surface, and depending on the plane of cut, highly variable features. Sections cut distantly from the center often revealed no submucosal diverticula nor communication with the surface.

Sections cut nearer the center revealed diverticula varying widely in number, size, and shape. Many were located high in the complex, very near the overlying muscularis mucosae, but some extended deeply, even reaching the connective tissue "capsule" below. Some had narrow lumina, others expanded and wide. Many contained mucus; intraluminal cells, cellular debris, or exudates were present on occasion. Though they frequently lay close to follicular germinal centers, diverticula were never observed within one.

Sections cut parallel with the luminal surface greatly facilitated appreciation of the radial pattern assumed by the tubular epithelial diverticula ramifying outward into the lymphoid tissue of the complex (see Figure 6).

Diverticula were tight and narrow at the level of the muscularis mucosae, but broadly expanded at their termini. Occasional diverticula bifurcated.

The well ordered circular collar of smooth muscle which encircled the diverticula as they entered the submucosa was formed by a downward backfolding of the muscularis mucosae. Its tightly bundled and

Figure 7. Two epithelial diverticula within the internodular lymphoid tissue of the LGC depicted in Fig. 6; this section lay between a) and b) of Fig. 6. The normal well ordered cuboidal to columnar pattern of the epithelium is disturbed by the presence of numerous intraepithelial leukocytes with dark nuclei and lighter cytoplasm. X 408

Figure 8. Oil immersion of same area seen in Fig. 7. Distinctly taller microvilli are just barely perceptible along the surface of an epithelial cell enclosing an intraepithelial leukocyte (arrow). This cell presumably represents the same type depicted in Figs. 15 and 18. Short regular brush borders are visible to either side of the indicated cell. X 1170

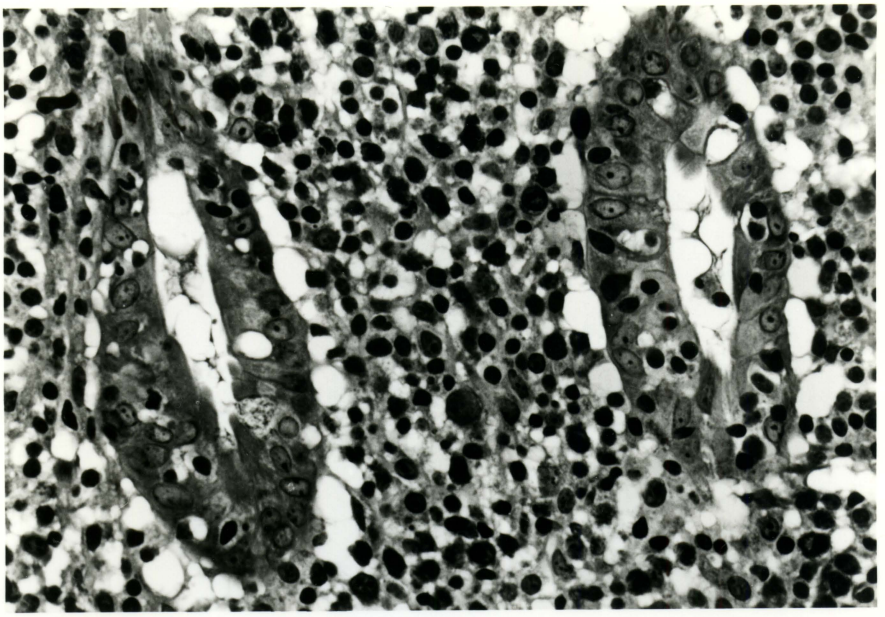

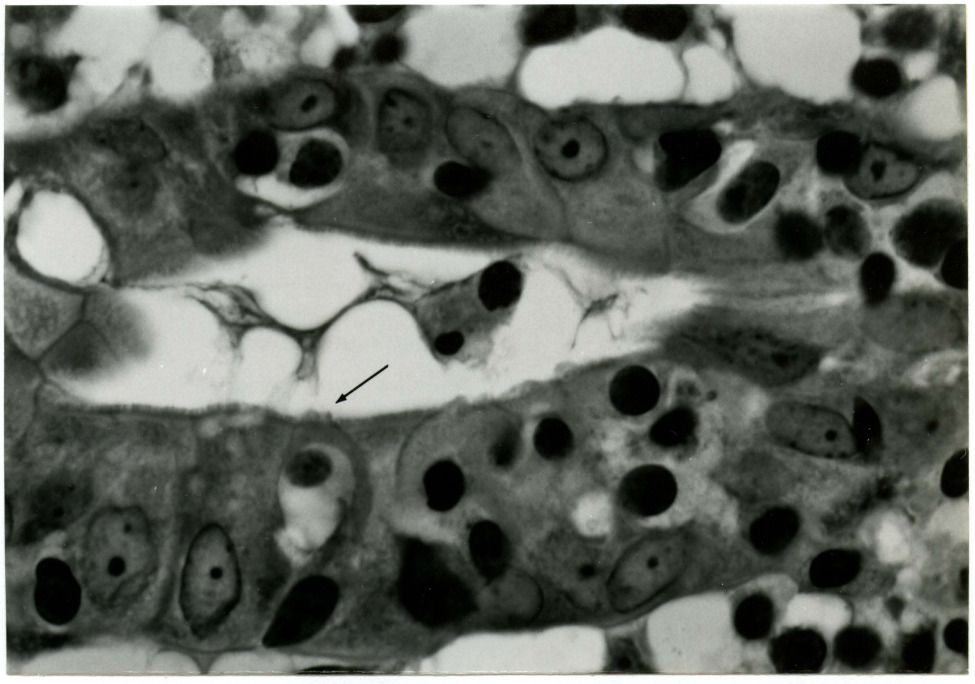

uniformly parallel fibers contrasted sharply with the loosely interwoven pattern of the muscularis elsewhere. No muscle fibers were observed within or beneath the connective tissue capsule enclosing the lymphatic nodule(s).

By light microscopy, identifiable cells in the diverticular epithelium included cuboidal to columnar epithelial cells, goblet cells, intraepithelial leukocytes (sometimes clustered), and occasional cells with unusually tall microvillous borders (see Figure 8).

Goblet cells were plentiful in some areas, but scarce in others. The epithelium appeared highly disordered in areas of prominent leukocyte infiltration.

Scanning electron microscopy

In colon dilated by intraluminal fixation, LGCs were variably elevated, volcano-like forms scattered across the colonic mucosa (see Figure 9). Usually a central pore was present, though in some the central region was elevated to form an irregular plateau. The large pores contrasted strikingly with typical crypt orifices or the tiny pits resulting from goblet cell discharge (see Figure 10).

The cut edge of vertically sectioned specimens revealed interior structure coinciding with the histologic impression (see Figures 4 and 11). Multiple, closely packed, epithelial diverticula passed through a gap in the muscularis mucosae and extended out and down into the lymphoid tissue below. The thick blunt collar of smooth muscle folding back on itself was readily visible (see Figure 12). Cross-cuts of diverticula confirmed the variability in location, extent, and lumen

Figure 9. LGCs as seen on the luminal surface of the proximal spiral colon of an 11-week old pig. Transected edge of the colon wall is visible at the lower extreme. Infusion fixed with glutaraldehyde. SEM. Bar=1mm

Figure 10. Pore representing locus of epithelial penetration down to and beneath the muscularis mucosae. The pore is much larger in diameter than the orifices of mucosal glands (arrow) or the pits left after goblet cell (arrow head) discharge. This LGC shows less elevation than those of Figure 9. SEM. 6-week old pig; distal spiral colon. Bar=200um

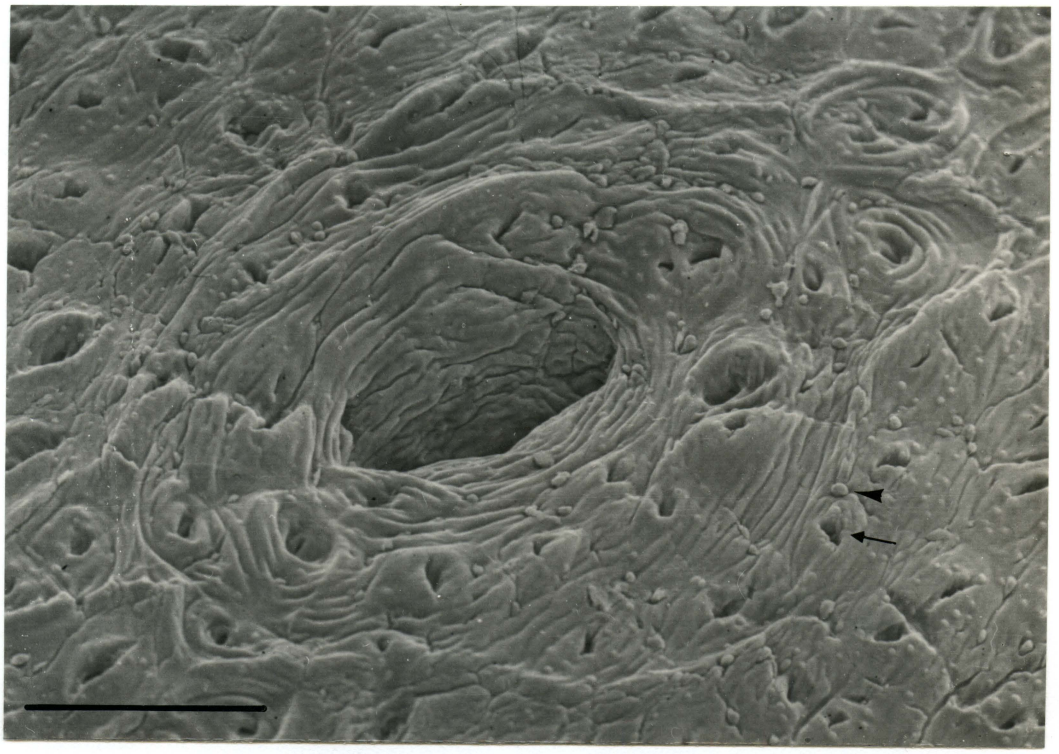

Figure 11. Bisected LGC. SEM. Slight elevation, central surface pore, multiple epithelial diverticula passing between folds (f) of muscularis mucosae, and dilated extremeties of diverticula (e) within the lymphoid tissue are all visible. Lumen of a vascular channel (v) is visible just to right of a connective tissue capsule enclosing the LGC and just below the muscularis mucosae. Lumens of bases of several mucosal glands (g) are seen just above the muscularis mucosae. 6-week old pig; proximal spiral colon. Bar=500um

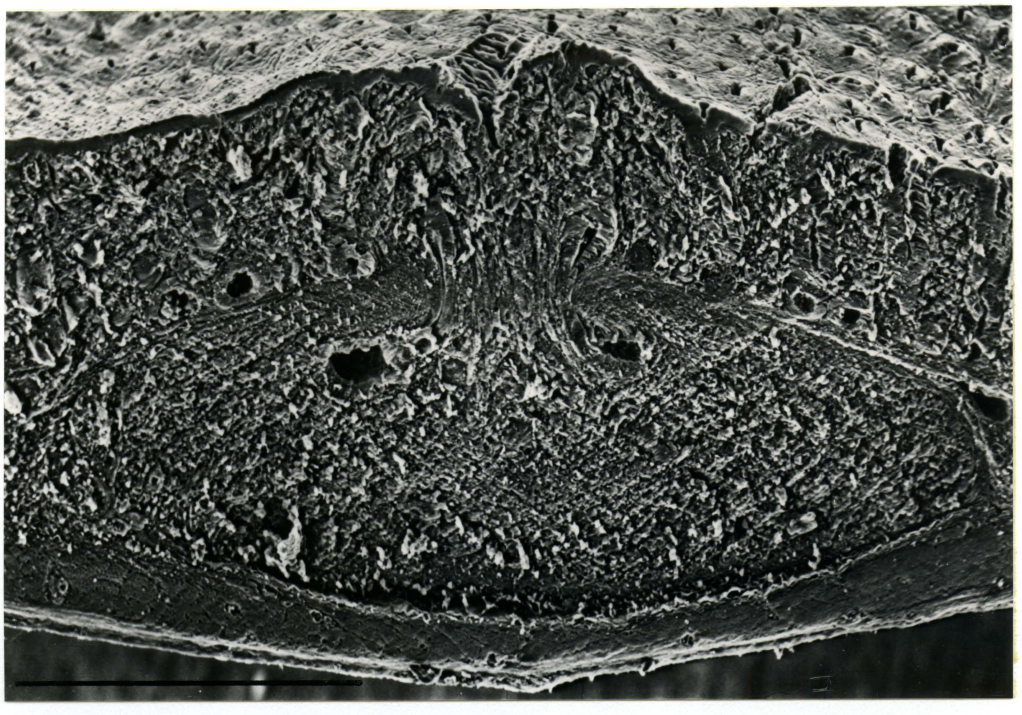

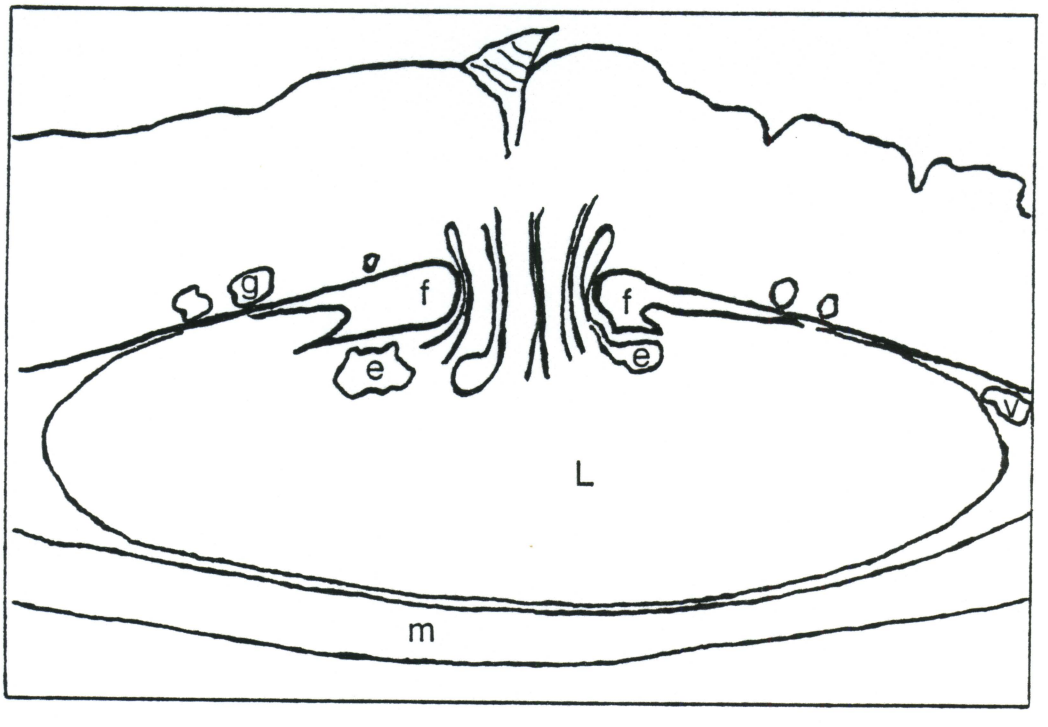
g
f
f
e
e
L
m

Figure 12. Higher magnification at the level of the gap in the muscularis mucosae as shown in Fig. 11. An epithelial diverticulum lies tightly against the fold of the muscularis mucosae as it passes and enters the lymphoid tissue below. Lymphocytes lie between the smooth muscle bundles peripheral to the fold proper (arrow). Mucin droplets are visible within goblet cells of surface glands (arrowhead) and the diverticulum (double arrowheads; see Fig. 16). The lumen of a neighboring diverticulum is seen at the lower right corner. 6-week old pig; descending colon. SEM. Bar=100um

Figure 13. Surface epithelium along the margin of the pore of a LGC in the descending colon of a 10-week old pig. Numerous cells bearing taller microvilli are interspersed among typical surface epithelial cells with short dense microvillous lawns. A partly discharged goblet cell is present at the upper left; another with a bulging surface is at the bottom left. SEM. Bar=10um

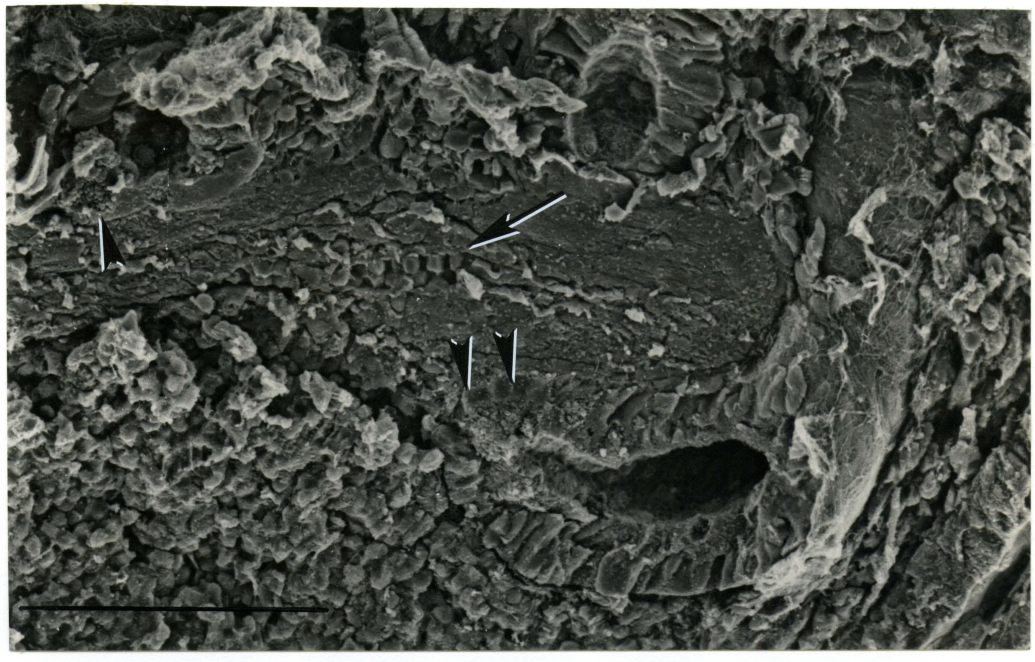

Figure 14. Higher magnification of the cell located near the center of Fig. 13. The taller microvilli are discrete and round. They are free of the fine material which overlies the shorter microvilli (presumably mucin). SEM. Bar=2um

Figure 15. LGC diverticular epithelium. A cell bearing tall microvilli very similar to those in Figure 14 is present among others with shorter and more tightly packed microvilli. The tall microvilli appear to be slightly coarser than the shorter type. Descending colon of same pig as Fig. 13; different LGC. SEM. Bar=2um

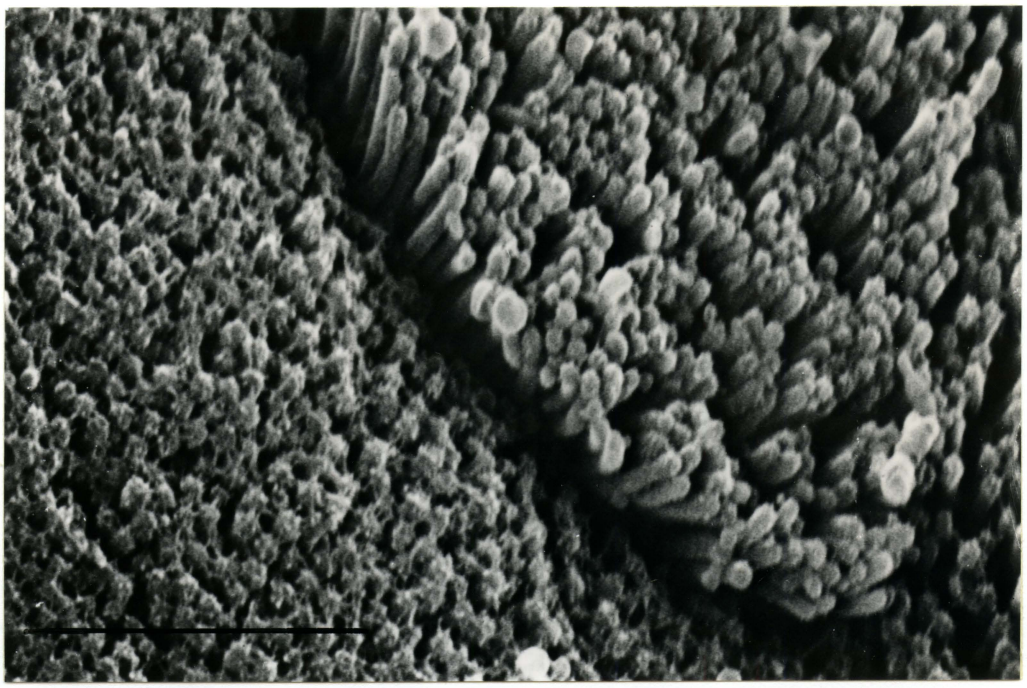

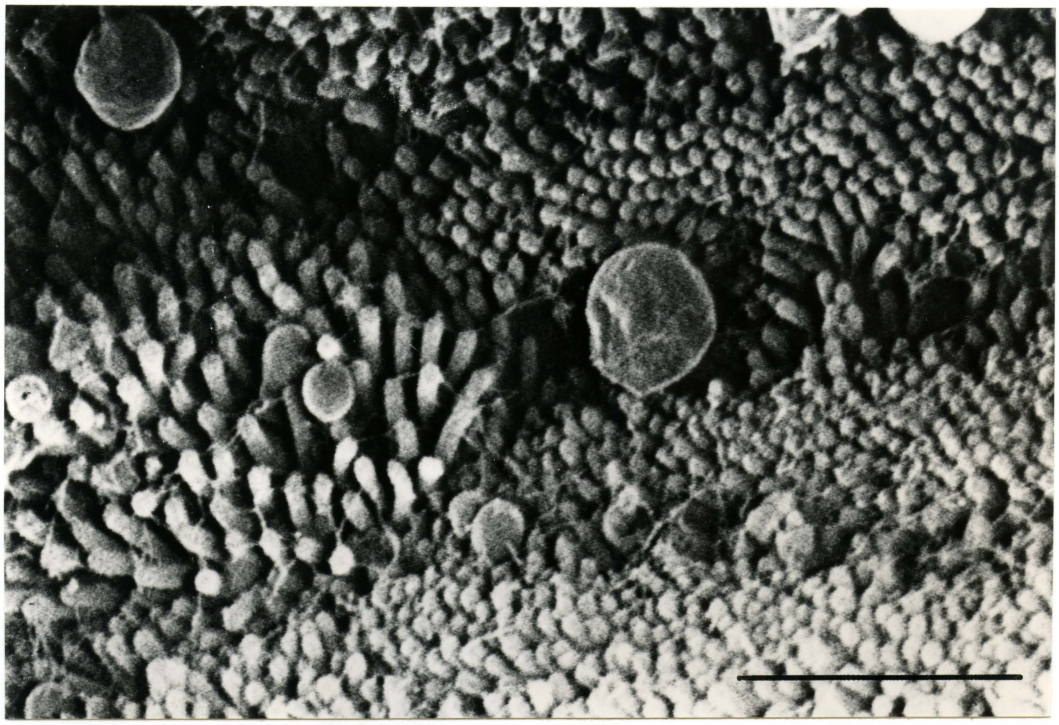

Figure 16. Sparse and stubby microvilli covering a diverticular epithelial surface rich in goblet cells (see Fig. 12). Surfaces of some goblet cells are open; others (arrow) bulge upward and show thinning of microvilli. SEM. Bar=10um

Figure 17. Diverticular epithelium composed primarily of cells covered with densely packed microvilli overlaid with and obscured by material similar to that seen in Figs. 13 and 14. Occasional goblet cells bulge above neighboring cells. SEM. Bar=50um (left); right side is 8X higher magnification (same bar=6.25um)

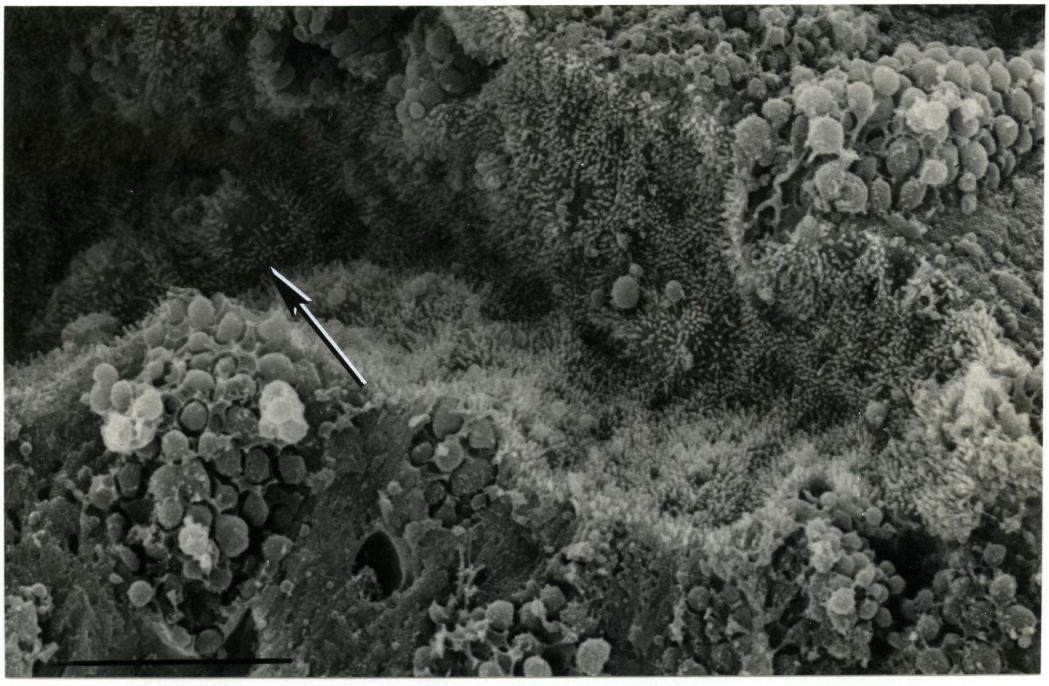

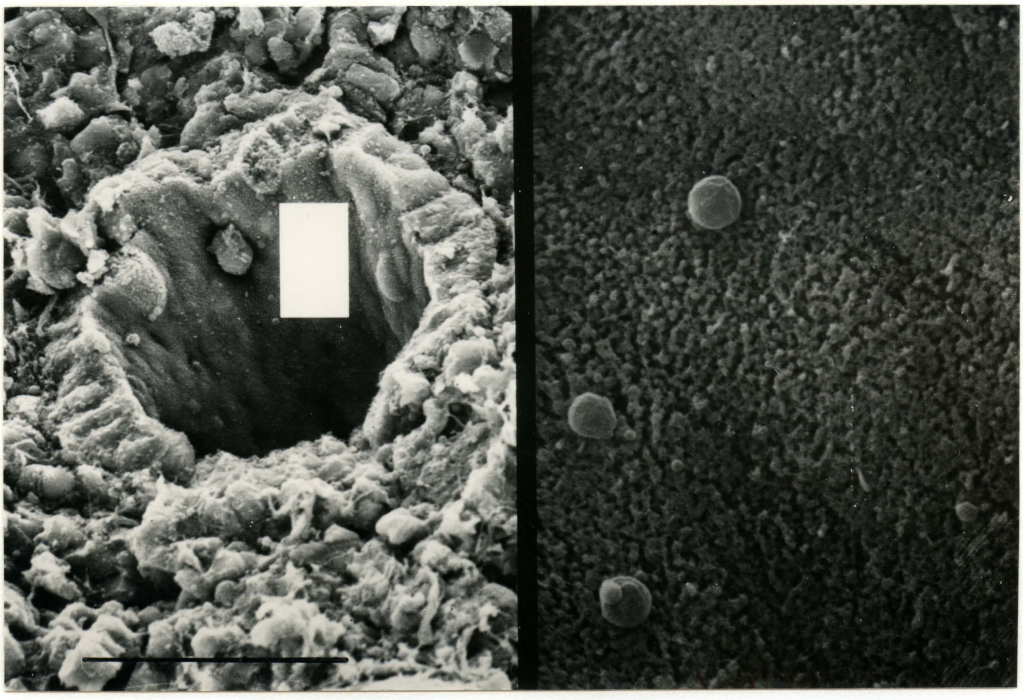

circumference observed histologically.

Goblet cells, with their large mucin droplets either bulging to the surface or along cut edges, were numerous in some areas but scarce in others (see Figures 16 and 17).

Microvillous patterns were apparent at higher magnification. They ranged from dense and tightly packed, very similar to those of surface epithelium, to more open and scant, but yet evenly distributed populations of stubby microvilli. Some cells with stubby microvilli could be identified as goblet cells. (See Figures 15-17.)

Cells with angular outlines and tall and coarse microvilli were seen on specimens from one animal (see Figures 13-15). This cell type was not restricted to the diverticula of the complexes but was found in surface epithelium as well. One to a few of such cells forming small patches were irregularly distributed among columnar epithelium and goblet cells.

Transmission electron microscopy

Detailed differentiation between diverticular epithelial cell types was possible ultrastructurally. At least five types of "native" cells were distinguishable (1-5 below), and both lymphocytes and macrophages were present intraepithelially (intraepithelial leukocytes; IELs).

1. Goblet cells (see Figures 18 and 23) were recognized easily by their large aggregates of mucin droplets. Their microvilli were distinct, but few in number, being most plentiful peripherally (bulging droplets of mucus generally obliterate surface features centrally). Goblet cells were rare or absent in some regions of diverticular

epithelium.

2. Cells with abundant, membrane bounded, uniformly electron dense cytoplasmic granules and prominent rough endoplasmic reticulum were found both immediately adjacent to the basement membrane and midway through the epithelial layer. Granules varied somewhat in size, but were homogeneously electron dense. These cells were interpreted as enteroendocrine cells (see Figure 19).

3. In a 10-week old pig, cells possessing unusually tall and coarse microvilli were found. Core filaments of the microvilli extended far deeper into the apical cytoplasm than in other cell types. Distinct microvilli might be locally or totally absent, and the apical (luminal) cell membrane was often very irregular, with thick pseudopod-like projections arising from it. Numerous surface pits (some clearly "coated") and small vesicles and membrane bounded tubules were present in the apical cytoplasm. Intraluminal leukocytes were present in close association to the apices of these cells. (See Figures 18, 20, and 23.)

Many of these cells contained large, membrane bounded inclusions. The inclusions contained numerous irregular, flocculent, partially membrane bounded, electron dense masses intermingled among multitudes of smaller (28-70 nm), pleomorphic, membrane bounded spherules with variably electron dense interiors (see Figures 20 and 21). Similar aggregates were present adjacent to these cells in the intercellular space of the epithelium and beneath the basement membrane adjacent to leukocytes of the lymphoid tissue (see Figure 18).

Nuclei were often deeply indented or folded.

Figure 18. TEM, montage. Epithelial diverticulum of LGC from the proximal spiral colon of a 10-week old pig. FAE region. M cell-like cells 1) possess irregular surface membranes (tall coarse microvilli=a, pseudopod-like forms=b, or smooth areas=c); 2) contain deeply indented nuclei (N) and 3) contain membrane bounded aggregates (A) of small vesicles and flocculent electron dense material bounded by membrane remnants. Similar material is present both between cells (arrow) and beneath the basement membrane (double arrows) where it is partly engulfed (arrowhead) by cytoplasmic processes of an adjacent cell. Intraepithelial leukocytes (L) lack desmosomal attachments typical of native epithelium. A leukocyte squeezes through a small opening between the bases of two epithelial cells (star). Portions of cells, most likely leukocytes, are in the diverticular lumen. Goblet cell, G. X 3015


L
N
A
L
a
b
L
c
N
G
A

Figure 19. Section of LGC diverticular epithelium, descending colon, 11-week old pig. Enteroendocrine cell with variably sized, but uniformly electron dense granules is positioned midway between the basement membrane and the luminal surface. RER, prominent in the apical cytoplasm, is abundant relative to neighboring epithelial cells. Note the scarcity of microvilli and their irregular orientation on nearby cells and the extensive interdigitation of lateral membranes; nuclear outlines are also very irregular. To the right of the enteroendocrine cell are two small portions of cells with very pale cytoplasm, probably representing IELs. TEM. X 6400

Figure 20. Group of cells located at the recess of the epithelial fold shown in Fig. 18. Small membranous vesicles and flocculent material are contained within large intracytoplasmic membrane bounded vacuoles (A) and beneath a desmosome (arrow) in the intercellular space. The surface of the cell bearing these inclusions is irregularly folded with microvilli laid sideways within a pocket of apical membrane. Apical cytoplasmic vacuoles are prominent in this cell and the cell adjoining the goblet cell. Interdigitation of lateral cell membranes is prominent. Mucin escapes from the apex of the goblet cell. TEM. X 12,400


A

Figure 21. Higher magnification of the large inclusion in the cell discussed in Fig. 20 (as viewed on the section depicted in Fig. 18). Bilayered membranes enclose the inclusion (arrow), encircle the vesicles (arrowhead), and partially bound the larger aggregates of flocculent dense material (double arrows). Desmosome (D) with radiating tonofilaments. Mitochondrion (M) is swollen. TEM. X 56,300

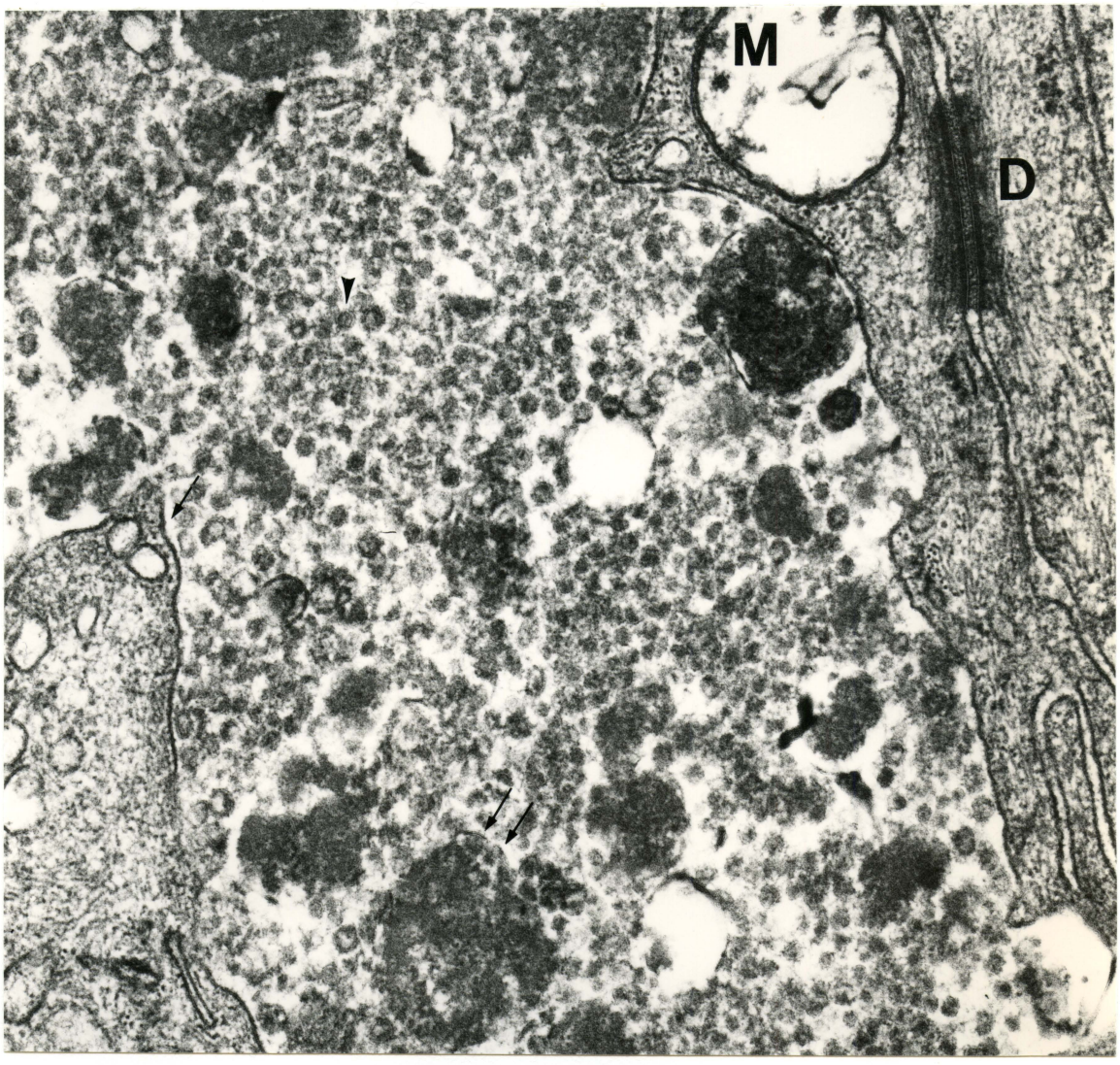
M
D

4. Cuboidal epithelial cells were common, especially in areas containing few goblet cells (see Figure 22). Nuclei were often contorted and indented, and large relative to the cell size. Microvillous borders were poorly developed. Those few present were short and often inclined at varying angles to the cell surface. Core filaments and rootlets of the microvilli were indistinct and sometimes not visible at all. Coated pits could be found along the surface and basal membranes. Cytoplasmic organelles such as mitochondria were occasionally present very near the apical membrane of the cell; an apical terminal web was not distinguishable. Variably electron dense granules enclosed by membranes either closely apposed to or partly separated from core material, suggestive of secretory granules, were sometimes present. IELs, individual and clustered, were often found among these cuboidal cells.

The cuboidal epithelium was reminiscent of basal cells of surface crypts. They too possessed only few, short, irregularly oriented microvilli. Core filaments and rootlets, however, were distinctly more well developed and secretory-like granules were routinely present.

5. Columnar epithelial cells with thickly packed, orderly, and tall microvillous borders were also present (see Figure 23). Core filaments were prominent. Granules (see 4. above) might be present at the apical end of the cell. IELs were found among these cells too.

Microvilli of these cells were similar ultrastructurally to those of the surface epithelium; all had prominent, dense core filaments and deep rootlets. The terminal web region was devoid of organelles.

Figure 22. Region of cuboidal diverticular epithelium from a diverticulum located deep in a LGC, proximal spiral colon, 6-week old pig. Microvilli are irregularly arranged over the surfaces of the cells; core filaments are present, but not prominent. Small vacuoles are present in the apical cytoplasm. Dark cores fill granules in the lower regions of the cells, but are eccentrically placed in those near the surface (upper center). Lateral membrane interdigitation is extensive. An IEL is situated between other epithelial cells at the lower left; presence of a phagosome-like inclusion suggests the cell is a macrophage. Folds indent the nucleus at the upper right. TEM. X 9855

Figure 23. Portion of LGC diverticular epithelium, proximal spiral colon, 10-week old pig. M cell-like cells with irregular surfaces or disordered and coarse microvilli (M). Apical vesicles are prominent in some of these cells (arrow). Microvilli are dense, uniform, and well ordered on an adjoining epithelial cell (E) and goblet cell (G). A small portion of an IEL is visible (L); note absence of desmosomes. Intraluminal leukocyte is closely apposed to M cell-like cell (arrowhead). TEM. X 9000


G
E
L
M

IELs were present individually and in clusters randomly throughout the diverticular epithelium. They were found in association with most of the cell types described above, but were least frequently encountered in regions with many goblet cells, and most frequently found together with cuboidal cells and the cells covered with coarse microvilli and irregular surface membranes. In some instances they appeared well accommodated, fitting into widened areas of the intercellular space without significant distortion of adjacent cells. At other times the epithelium was disrupted and disordered. It was not unusual to find these leukocytes fixed in place while crossing the epithelial basement membrane (see Figure 18).

IELs were electron lucent relative to native epithelial cells and contained few cytoplasmic organelles (mitochondria were most common, but not numerous). A few contained membrane bounded structures consistent with lysosomes and phagolysosomes. These cells were considered macrophages and the remainder of lymphocyte origin.

A consistent feature of all epithelial cells was highly complex interdigitation between adjacent lateral membranes. It occurred between epithelial cells and IELs too, though not as extensively. Tight junctions and desmosomes were prominent between epithelial cells, especially near cell apices.

Quality of fixation was variable and not optimal in many of the tissues examined. This was evident from the severely swollen mitochondria and dilated endoplasmic reticulum and perinuclear spaces in some submucosal epithelial cells. Electron dense amorphous coagula,

perhaps representing condensations of membrane, were found within mitochondria and along cell margins. Subepithelial lymphoid cells often appeared distorted and surrounded by increased clear space. Cells of interest were adequately preserved, however, to display their basic morphological features.

DISCUSSION

Count and Distribution

The high number of LGCs present, their consistent distribution patterns, and their consistent morphology clearly substantiate the discrete (solitary) submucosal lymphoglandular complex as a prominent, well defined, and normal component of the porcine colon.

Sample size was small: two separate litters with three replicates (pigs) of each. Even so, the difference between litter mean counts does not approach significance ($p<0.1$) by Student's t (58). Increased sampling should only reduce further the small variability already encountered.

Count results are consistent with those reported from younger pigs using the same technique where means of 959 and 1149 per colon were established in 4- and 6-week old piglets respectively (increased from 520 in 1-week old animals) (27). Here, 1068 LGCs in the 5-week pig and a range of 1068 to 1499 and mean of 1231 between five and thirteen weeks of age (n=6) correlate with the former.

Figures reported from an earlier study (7) of porcine colon are overall lower (325-791 total) but age of animals is unspecified. That technique employed fresh, unstained intestine, serosal stripping, and viewing by transmitted and reflected light.

In the only report found from a non-porcine species, 2351 and 4618 "lymphoid nodules" were counted in two whole human colons (16).

Methylene blue staining of colons fixed in acetic acid was

successful from the outset and overcame early difficulties with identification of lymphoid tissue (see Appendix C). Persistent, intense, and selective staining of LGCs was achieved.

The prolonged wash in cold water produces a very clean and firm specimen. Fixation in acetic acid hemolyzes any residual red blood cells and induces marked tissue swelling (especially collagenous tissue) (48, 57). Both of these effects contribute to a remarkably translucent specimen in which the stained LGCs stand out clearly from the remainder of the bowel wall. Acetic acid precipitates nucleoproteins (48). The high concentration of nucleic acid in lymphoid nodules is responsible for their relatively intense staining (methylene blue is a cationic dye).

All processed colons were suitable for counting of LGCs regardless of processing parameters. Prepared specimens could be held refrigerated in small volumes of water for several days with no loss of quality. In fact, one to two days storage actually enhanced differentiation since superficial non-specific stain precipitates tended to fall away.

Counting all LGCs present in whole colons was necessary in light of observed differences in counts between different regions of colon (see Appendix C). Results here bear out those differences, but the uniformity between animals was unexpected.

Early work on human colons revealed an overall mean density of 3.3 "lymphoid follicles" per square centimeter of bowel wall. Regional densities increased by 11, 26, and 29%, respectively, from the ascending to transverse, descending, and sigmoid colons (16). Later, figures of

3.4, 3.6, 3.5, and 3.8 were reported for the same four segments, respectively (29). These are broad divisions and counts were obtained from small "representative" specimens; this approach would mask gradual variations between regions. The results are nonetheless very uniform, and when two entire colons were inspected and all "follicles" counted, representative segments were judged valid as approximations (16).

A similarly conducted study of porcine colon indicated that relative frequency of "submucosal glands" increases from 0 at the cecocolic junction to a maximum somewhere between the colon and rectum and then declines again through the rectum (24). Absolute numbers are not provided.

In another study, in which porcine colons were divided into five portions of equal length, only ranges of counts are reported for each portion. Fewest were found in the proximal fifth; comparisons between other regions cannot be made. Though high variability between segments is reported, it is not indicated if a consistent pattern existed among animals (7).

In a relatively recent report, "lymphoid follicle" density in the porcine colon decreases from 34.7 to 17.9 per 10 cm^2 of bowel wall between one and six weeks of age; figures for rectum are 32.8, 43.4, and 28.5 at one, four, and six weeks of age respectively (27). Though an overall decline of density by age is obvious, regional distinctions are unclear. Close inspection of the report indicates that descending colon was likely included with "rectum", artificially lowering the "colon" count and raising the "rectum" count. (Note the highest increment in

the graph of the 5-week old pig in Figure 3. It represents the entire descending colon, 14 cm in length.)

The possibility of an age associated increase in total LGC number cannot be disregarded (see Table 2); only the total count (1043 LGCs) of the second 13-week old pig departs from such a pattern. However, the common distribution pattern depicted in the graphs in Figure 3, the progressive increase in eveness of distribution, and the insignificant differences in overall counts may suggest a more or less established number of LGCs which become more evenly distributed as the colon enlarges and assumes its mature proportions.

Light Microscopy

Morphological uniformity

"Lymphoglandular complex" implies specifically a structure characterized by both lymphoid and epithelial components. "Lymphoid nodule" is less restrictive, indicating only that a discrete aggregate of lymphoid cells is present; other features are not considered. The nodule is discernible grossly. Intimate epithelial association is definable only microscopically.

Submucosal lymphoid nodules are encountered during routine histological examination of porcine colon. Epithelial diverticula are present in some; in some they are not. Evidence of communication with the surface may or may not be present. In this study central pores could not be seen under low power magnification in a small percentage of LGCs during counting. This suggested that either two types of lymphoid

structures existed, those with and those without an epithelial component; or, alternatively, that the epithelial component of some was simply missed on examination.

As shown in Table 4, 35 of 36 specimens contained diverticula. This suggests that a high percentage of lymphoid aggregates observed by the methylene blue technique are true lymphoglandular complexes and that simple lymphoid nodules are rare. The evidence is limited, however, and needs to be validated.

Animals between four and thirteen weeks of age were used in this study because diseases associated with altered LGCs typically occur in this age group. This design, plus the small number of animals used, does not investigate at what point the colonic LGC develops nor firmly establish if there is a "fixed" number present once a certain age is attained. Influence of disease on number of LGCs present is also unknown. A recent report on human tissues claims an increase in number in diseased colons (41).

Histologic structure

The lymphoid component of the LGC is both well organized and regionally differentiated. Abundant internodular lymphoid tissue, distinct germinal centers, and overlying coronas against which epithelial diverticula lie qualify the complex morphologically for inclusion with "specialized amplification elements of the immune system" or GALT, in this case. As part of the "germinal center system", the complexes would serve as sources of memory B cells programmed to home to the lamina propria of mucus membranes throughout the body, as sites of

lymphocyte surface immunoglobulin switching (e.g., IgM to IgA), and as amplification sites for uncommitted B cells (63).

This is not a novel consideration, as the analogous structure in the human colon has been interpreted as "...a local receptor of antigenic material for future immune recognition" (30). Colonic lymphoid patches of the rat provide for "...efficient sampling of colonic luminal antigens, allowing sensitization..." (8).

Nonetheless, the colonic LGC, as a unique subentity of GALT, is generally given only cursory mention in discussions of organized mucosal lymphoid tissues (5, 43).

Unique follicle associated epithelium (FAE) of the mouse Peyer's patch, rabbit appendix, and chicken bursa of Fabricius are described as lower, free of goblet cells, and distorted or flattened due to subjacent lymphoid proliferation and intraepithelial infiltration (9). Similar descriptions are given for the FAE of the calf (31) and porcine (13) Peyer's patches noting, in addition, the tendency of IELs to cluster. Avian and mammalian BALT lymphoepithelium contains few goblet and ciliated cells and many lymphocytes in contrast to adjacent bronchial epithelium (6). FAE of the rat colonic lymphoid patch lacks mature goblet cells and contains clustered lymphoid cells (8). IELs cluster in the FAE of the rabbit appendix (54).

"Location of M cells can be inferred when groups of lymphoid cells are seen in follicle epithelium...;" and interestingly, basal and lateral membranes of M cells have greater affinity for lymphocytes than for enterocytes (44). But the relationship between resident epithelial

cells and intraepithelial lymphocytes may be more than one of simple spacial convenience. Intraepithelial lymphocytes can induce Ia antigen expression in Ia-negative intestinal epithelial cells and inhibit growth of these cells (12). There appears to be biochemical as well as physical interdependency between them. Ia-positive dendritic cells are also present in close contact with M cells, and possibly function in antigen presentation (65).

Significant features of the epithelial component of LGCs in the present study include intimate association with underlying lymphofollicular structures, focal areas of disruption with leukocytic infiltration, and extensive areas containing few goblet cells and cuboidal epithelium.

Serial sectioning established unequivocally that diverticula and mucosal communication were present. Alternatively, by precise bisection of complexes through the central pore and careful sectioning, diverticula and gaps in the muscularis mucosae were readily found.

Thus, the form and composition of the porcine colonic LGC, especially when correlated with the ultrastructural features discussed below, are that of a typical FAE with its antigen transport capacity (M cells).

Sectioning LGCs parallel with the mucosal surface made clear the radial diverticular pattern. Several serial sets all showing this same pattern imply that it is a uniform feature of all LGCs.

The smooth muscle collars arising from the muscularis mucosae and encircling the diverticula as they pass from mucosa to submucosa are

exceptionally thick and well ordered. They in fact seem too prominent to represent bundles of muscularis mucosae simply pushed aside. The collars are presumably capable of contraction.

Constriction would draw the outer connective tissue "capsule" of the LGC together and compress the interior. This would effectively eject any fluid content from the interior: ingesta, mucus, and secretions from the diverticula to the lumen proper of the intestine; and lymph and blood to their respective collecting lymphatics and venules. With relaxation, flow would occur in the opposite direction: a new sampling of lumen content would be drawn into the diverticular lumen and fresh lymph and blood would accumulate interstitially and intravascularly.

Assuming that the smooth muscle of the collars is functionally integrated with that of the rest of the muscularis mucosae, it seems plausible that its continuous, rhythmic contractions would cause such cyclic intake and discharge, the whole LGC thus serving as an active interface between the animal's inner and outer environments. Antigenic substances in the gut lumen would be continually brought within a single cell layer of a lymphoid organ (i.e., GALT) capable of functions such as: 1) formation of sensitized T cells, leading to both specific local cell mediated immunity and development of helper/suppressor cells 2) priming of B cells (immunocyte production) and 3) non-specific, germinal center B cell amplification (63).

Electron Microscopy

Scanning

Low power views of the LGC, both intact and sectioned for interior viewing, permit immediate appreciation of the complex's three-dimensional form. The importance of dilating the intestine for localization of the complexes is emphasized.

Microvillous patterns are well defined at higher magnifications and correlate with TEM results (below). Dense tight brush borders correspond to the regular, uniform, "surface-like" pattern seen by TEM. The more open pattern may represent either the cuboidal epithelium with its sparse microvillous surface or goblet cells. It is unclear if goblet cells possess fewer microvilli inherently or if the brush border is artificially thinned due to surface expansion caused by mucus accumulation.

The scattered cells with taller and coarser microvilli share features with both tuft cells (38) and cells previously designated as M cells (60). Ultrastructural features are discussed below.

Overall, SEM proved to be of limited value in fine definition of the epithelial layer. Firstly, very little diverticular surface area is available for inspection on most specimens. Longitudinal cuts through a diverticulum are rare. Simple cross-cuts usually result, but are also infrequent and unpredictable, and of little value since only the outermost tiers of epithelial cells can be illuminated with the beam. Secondly, firm definition between some cell types is not possible.

Considered, but not yet carried through, are attempts to finely

section the mucosa of specimens in the plane of the wall of the intestine. If achieved at the proper depth, a large number of diverticula could be "laid open" on a single specimen, enhancing the utility of SEM.

Transmission

Ultrastructural examination of epithelium from LGC diverticula reveals a heterogeneous population of cells. Cellular composition varies between diverticula and probably within a given diverticulum. Areas of FAE-like epithelium are apparently interspersed among others devoted more so to mucin production, secretion, or cell renewal. A basis for this segregation awaits clarification, as do the roles of age, immune status, and disease on the relative extent and activity of FAE-like versus non-FAE regions.

M cells from porcine Peyer's patch dome epithelium, in comparison to neighboring columnar epithelial cells, reportedly possess fewer and larger, or irregular, thick, and loosely arranged microvilli; some of these contain microfilaments. Blunt cytoplasmic projections extend from the apical surface. Lateral interdigitations and desmosomes are abundant. Cytoplasmic vesicles are not prominent. Nuclei are indented (13).

Cells with these same features were identified in some areas of colonic LGC epithelium. In contrast to porcine Peyer's patch M cells (13), they were not consistently less electron dense than other epithelial cells; IELs were usually less electron dense than resident epithelial cells.

Though in an early report (46) microvillous core filaments are entirely absent from surface microfolds of human Peyer's patch M cells, in a later study of rat Peyer's patches filaments are prominent in M cell microvilli (35). In the FAE of rat colonic lymphoid patches, microvilli and terminal webs are "normal" (8). Prominence of microvillous features such as number, regularity, and branching probably vary with the degree of maturation of the cell (11). Photomicrographs (11) suggest that microvillous height and core filament formation are also diminished in mature versus immature M cells. Core filaments and rootlets of Peyer's patch M cell microvilli may appear very similar to those of adjacent enterocytes (as published in Figure 8 of 44).

Cells of dome FAE of calf Peyer's patches are described as containing apical vacuoles and other multivesicular bodies containing membrane fragments and opaque bodies with indistinct particulate and membranous contents (residual bodies). Some of these vacuoles are seen communicating with the intercellular space (31). Particulate material from the intestinal lumen is reported in large cytoplasmic vacuoles of FAE cells (M cells) from Peyer's patches of normal and rotavirus infected calves and between FAE cells of infected calves (61). This configuration is virtually identical to that presently observed in the diverticular epithelium of the porcine colonic LGC.

The presence of numerous leukocytes in diverticular lumens bordered by M cell-like cells is consistent with the suggested role of M cells as sites of lymphocyte transepithelial diapedesis (45). It is even postulated that leukocytes may be actively conveyed across

lymphoepithelium by contractile movements of resident epithelial cells (53).

Though strong morphological evidence was found supporting the colonic LGC diverticular epithelium as another site of GALT FAE with specialized antigen transport cells, firm proof awaits functional studies using tracer materials. Only then may proven functional characteristics of FAE such as unique antigen specific adherence (8, 70, 71), uptake (3, 8, 9, 14, 32, 36, 39, 42, 47, 61, 67, 70, 72), transport to inter- and subepithelial zones (9-11, 14, 33, 36, 42, 47, 51, 61, 67, 69, 70), and cell-to-cell conveyance (42, 70) be established for this lymphoepithelial organ as well.

Such studies should also be of value in resolving whether cells possessing tall and coarse microvilli, or those with irregular surfaces and blunt processes, are tuft cells, antigen transport cells (M cells), or both.

Though tissues were adequately preserved to recognize and identify cell types and constituent organelles, evidence of hypoxic change or delayed fixation was present. Hypoxic change could result from either shock or local vascular embarrassment during tissue collection. The sequestered location of the LGC in the submucosa may delay fixation of the tissue. Glutaraldehyde penetrates tissue poorly and slowly. Use of combined glutaraldehyde-formaldehyde fixatives such as Karnovsky's (28) might hasten fixation after intraluminal infusion. Perfusion fixation is another alternative.

M cell surface membranes undergo artifactual alteration (formation

of surface vesicular membrane remnants) due to "lipid flow" when aldehyde fixation alone is employed (11). This might account for some of the marked surface irregularity seen in the M cell-like cells studied here, and selective distortion could even be viewed as an argument in support of an antigen transport character for these particular cells. Combined fixation with glutaraldehyde and osmium tetroxide eliminates remnant formation (11).

Finally, what significance is there in cataloguing the porcine colonic submucosal LGC as lymphoepithelial tissue, FAE, or GALT?

From a basic research perspective, it is hoped that any understanding gained here, whether in technique, recognition, or interpretation, might facilitate investigations of the same or analogous tissues in other sites or species.

"Peyer's patches constitute major sites where antigens from the gut lumen encounter immunocompetent cells and trigger events leading to immune responses (44)" or "...enteropathies such as allergic disorders and/or inflammatory bowel disease (18);" the same should hold true of colonic LGCs.

FAE serve as specific foci of infection for Salmonella (25) and reovirus 1 (70) in the murine Peyer's patch, M cells for the bovine astrovirus (71) in the Peyer's patch of the calf, and M cells again for E. coli (strain RDEC-1) in Peyer's patches of rabbit ileum (26).

LGCs in the porcine colon undergo marked change in many types of colitis (see Figure 24). Are certain diseases initiated at, focused on, or localized to the LGC because of its form, composition, or function?

Investigation of properties such as transport capacity, presence of surface enzymes and receptors, and pathogen adherence, localization, or uptake will help define the functional role of the complex and its participation in the pathogenesis or resolution of diseases involving it. Given the importance of colonic diseases in swine husbandry, fuller understanding of their pathogenesis is imperative in establishing effective schemes of diagnosis, treatment, and control, including vaccination.

Figure 24. LGC from the colon of a 13-week old pig experimentally infected 21 days earlier with Treponema hyodysenteriae. The lumen is cystically dilated by mucus and cellular debris. Goblet cell hyperplasia of diverticular epithelium is evident as well as a long cuboidal region devoid of goblet cells. Atrophy of the lymphoid component is striking. X 42

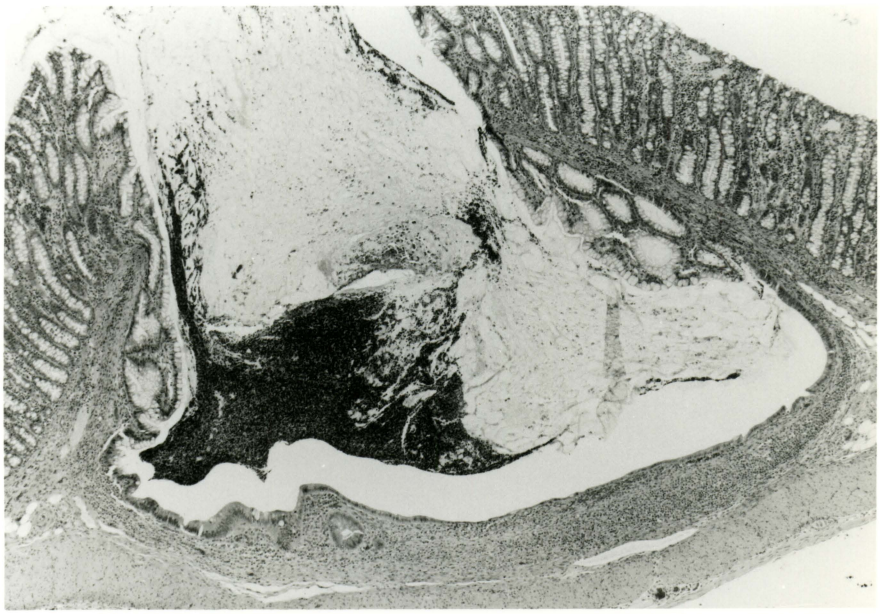

CONCLUSIONS

1. Porcine colonic submucosal lymphoglandular complexes (LGCs) are a normal and distinctive feature of the porcine colon. An average of 1231 were counted in colons of six pigs between five and thirteen weeks of age.
2. In pigs between five and thirteen weeks of age, colonic LGCs are grossly identifiable by cold water washing, fixation in acetic acid, and staining with methylene blue.
3. The entire porcine colon except the proximal 7-12% contains submucosal LGCs.
4. Area density of porcine colonic LGCs becomes more uniform across the entire length of the colon between five and thirteen weeks of age. In younger animals LGCs are more dense over the central regions. Maximum densities range from 45.4/10 cm^2 (5-week old pig) to 8.3/10 cm^2 (13-week old pig).
5. Virtually all lymphoid aggregates identifiable grossly in the wall of the porcine colon represent true LGCs.
6. Histologically, the colonic LGC consists of a well demarcated, partially encapsulated lymphocytic aggregate in the tela submucosa of the colon wall. Variable numbers of lymphatic nodules with germinal centers and coronas of small lymphocytes are included. A circular gap in the muscularis mucosae, usually indicated by a central pore-like depression of the surface epithelium, permits extensions of mucosal glands to penetrate the internodular lymphocytic tissue beneath. The epithelial diverticula spread

radially from the pore. They extend to variable depths, occasionally branch, and usually have dilated extremities. Goblet cells and cuboidal to columnar non-mucus cells comprise the epithelium and intraepithelial leukocytes, singly and in clusters, multifocally disrupt the otherwise orderly epithelium.

7. Cells possessing many ultrastructural features in common with known antigen transport epithelia are present in the porcine colonic submucosal LGC. LGCs are morphologically compatible with other varieties of mucosal lymphoid organs.
8. The colonic LGCs possess immense potential for immunological sensitization given the tremendous microbial and food antigen load of the large intestine.

LITERATURE CITED

1. Atkins, A. M., and Schofield, G. C. 1972. Lymphoglandular complexes in the large intestine of the dog. J. Anat. 113(2):169-178.

2. Barker, J. K., and Van Dreumel, A. A. 1985. The alimentary system. Pp. 1-237. In K. V. F. Jubb, P. C. Kennedy, and N. Palmer. Pathology of Domestic Animals. Vol. 2. 3rd ed. Academic Press, Orlando.

3. Beezhold, D. H., Sachs, H. G., and Van Alten, P. J. 1983. The development of transport ability by embryonic follicle-associated epithelium. J. Reticuloendothel. Soc. 34:143-152.

4. Bienenstock, J. 1984. The mucosal immunologic network. Ann. Allergy 53:535-539.

5. Bienenstock, J., and Befus, D. 1984. Gut- and bronchus-associated lymphoid tissue. Am. J. Anat. 170:437-445.

6. Bienenstock, J., McDermott, M., Befus, D., and O'Neill. 1977. A common mucosal immunologic system involving the bronchus, breast, and bowel. Adv. Exp. Med. Biol. 107:53-59.

7. Biswal, G., Morrill, C. C., and Dorstewitz, E. L. 1954. Glands in the submucosa of the porcine colon. Cornell Vet. 44:93-102.

8. Bland, P. W., and Britton, D. C. 1984. Morphological study of antigen-sampling structures in the rat large intestine. Infect. Immun. 43(2):693-699.

9. Bockman, D. E., and Cooper, M. D. 1973. Pinocytosis by epithelium associated with lymphoid follicles in the bursa of Fabricius, appendix, and Peyer's patches. An electron microscopic study. Am. J. Anat. 136:455-478.

10. Bockman, D. E., and Stevens, W. 1977. Gut-associated lymphoepithelial tissue:bidirectional transport of tracer by specialized epithelial cells associated with lymphoid follicles. J. Reticuloendothel. Soc. 21(4):245-254.

11. Bye, W. A., Allan, C. H., and Trier, J. S. 1984. Structure, distribution, and origin of M cells in Peyer's patches of mouse ileum. Gastroenterology 86:789-801.

12. Cerf-Bensussan, N., Quaroni, A., Kurnick, J. T., and Bhan, A. K. 1984. Intraepithelial lymphocytes modulate Ia expression by intestinal epithelial cells. J. Immunol. 132(5):2244-2252.

13. Chu, R. M., Glock, R. D., and Ross, R. F. 1979. Gut-associated lymphoid tissues of young swine with emphasis on dome epithelium of aggregated lymph nodules (Peyer's patches) of the small intestine. Am. J. Vet. Res. 40(12):1720-1728.

14. Chu, R. M., Glock, R. D., and Ross, R. F. 1982. Changes in gut-associated lymphoid tissues of the small intestine of eight-week-old pigs infected with transmissible gastroenteritits virus. Am. J. Vet. Res. 43(1):67-76.

15. Cornes, J. S. 1965. Number, size, and distribution of Peyer's patches in the human small intestine. Gut 6:225-233.

16. Dukes, C., and Bussey, H. J. R. 1926. The number of lymphoid follicles of the human large intestine. J. Pathol. Bacteriol. 29:111-116.

17. Dunne, H. W., Luecke, R. W., McMillen, W. N., Gray, M. L., and Thorp, F. 1949. The pathology of niacin deficiency in swine. Am. J. Vet. Res. 10:351-356.

18. Egberts, H. J. A., Brinkhoff, M. G. M., Mouwen, J. M. V. M., Van Dijk, J. E., and Koninkx, J. F. J. G. 1985. Biology and pathology of the intestinal M-cell. A review. Tijdschr. Diergeneeskd. 110:1085-1088.

19. Elias, H. 1947. Submucosal glands in the bovine ileum. Am. J. Vet. Res. 8:52-53.

20. Epstein, S. E., Ascari, W. Q., Ablow, R. C., Seaman, W. B., and Lattes, R. 1966. Colitis cystica profunda. Am. J. Clin. Pathol. 45:186-201.

21. Ferguson, H. W., Neill, S. D., and Pearson, G. R. 1980. Dysentery in pigs associated with cystic enlargement of submucosal glands in the large intestine. Can. J. Comp. Med. 44:109-114.

22. Glock, R. D. 1981. Digestive system. Pp. 130-137. In A. D. Leman et al., eds. Diseases of swine. 5th ed. Iowa State University Press, Ames.

23. Goodall, H. B., and Sinclair, I. S. R. 1957. Colitis cystica profunda. J. Pathol. Bacteriol. 73:33-42.

24. Hebel, R. 1960. Untersuchungen über das Vorkommen von lymphatischen Darmkrypten in der Tunica submucosa des Darmes von Schwein, Rind, Schaf, Hund und Katze. Anat. Anz. Bd. 109(1):7-27.

25. Hohmann, A. W., Schmidt, G., and Rowley, D. 1978. Intestinal colonization and virulence of Salmonella in mice. Infec. Immun. 22(3):763-770.

26. Inman, L. R., and Cantey, J. R. 1983. Specific adherence of Escherichia coli (strain RDEC-1) to membranous (M) cells of the Peyer's patch in Escherichia coli diarrhea in the rabbit. J. Clin. Invest. 71:1-8.

27. Inoue, T., and Sugi, Y. 1978. On gut associated lymphoid tissues of piglets. Bull. Fac. Agric. Yamaguti Univ. No. 29:21-29.

28. Karnovsky, M. J. 1965. A formaldehyde-glutaraldehyde fixative of high osmolality for use in electron microscopy. J. Cell Biol. 27:137A-138A.

29. Kealy, W. F. 1976. Lymphoid tissue and lymphoid-glandular complexes of the colon: relation to diverticulosis. J. Clin. Pathol. 29:245-249.

30. Kealy, W. F. 1976. Colonic lymphoid-glandular complex (microbursa): nature and morphology. J. Clin. Pathol. 29:241-244.

31. Landsverk, T. 1981. The epithelium covering Peyer's patches in young milk-fed calves. Acta Vet. Scand. 22:198-210.

32. Landsverk, T. 1981. Peyer's patches and the follicle-associated epithelium in diarrheic calves. Acta Vet. Scand. 22:459-471.

33. LeFevre, M. E., Vanderhoff, J. W., Laissue, J. A., and Joel, D. D. 1978. Accumulation of 2-um latex particles in mouse Peyer's patches during chronic latex feeding. Experientia 34(1):120-122.

34. Liebler, E. 1985. Untersuchungen zur Anzahl, Verteilung und Ausdehnung der schleimhauteigenen Solitärfollikel und Peyerschen Platten im Dünndarm des Kalbes unter besonderer Berücksichtigung ihrer Oberflächenstruktur. Dissertation, Tierärztliche Hochschule, Hannover.

35. Madara, J. L., Bye, W. A., and Trier, J. S. 1984. Structural features of and cholesterol distribution in M-cell membranes in guinea pig, rat, and mouse Peyer's patches. Gastroenterology 87:1091-1103.

36. Marcial, M. A., and Madara, J. L. 1986. Cryptosporidium: cellular localization, structural analysis of absorptive cell-parasite membrane-membrane interactions in guinea pigs, and suggestion of protozoan transport by M cells. Gastroenterology 90(3):583-594.

37. McNabb, P. C., and Tomasi, T. B. 1981. Host defense mechanisms at mucosal surfaces. Ann. Rev. Microbiol. 35:477-496.

38. Nabeyama, A., and LeBlond, C. P. 1974. "Caveolated cells" characterized by deep surface invaginations and abundant filaments in mouse gastro-intestinal epithelia. Am. J. Anat. 140:147-166.

39. Neutra, M. R., Guerina, N. G., Hall T. L., and Nicolson, G. L. 1982. Transport of membrane-bound macromolecules by M cells in rabbit intestine. Gastroenterology 82(5):1137. (Abstr.)

40. Nickel, R., Schummer, A., Seiferle, E., and Sack, W. O. 1973. The viscera of the domestic mammals. Springer-Verlag, New York.

41. O'Leary, A. D., and Sweeney, E. C. 1986. Abnormalities in frequency, distribution and lymphoid substructure of lymphoglandular complexes (LGC) in colorectal disease. Gastroenterology 90(5):1796. (Abstr.)

42. Owen, R. L. 1977. Sequential uptake of horseradish peroxidase by lymphoid follicle epithelium of Peyer's patches in the normal unobstructed mouse intestine: an ultrastructural study. Gastroenterology 72:440-451.

43. Owen, R. L. 1983. Ultrastructure of antigen trapping epithelia of mucosal lymphoid organs. In "Regulation of the immune response. 8th Int. Convoc. Immunol., Amherst, N. Y., 1982" (Karger, Basel) pp. 88-98.

44. Owen, R. L., and Bhalla, D. K. 1983. Cytochemical analysis of alkaline phosphatase and esterase activities and of lectin-binding and anionic sites in rat and mouse Peyer's patch M cells. Am. J. Anat. 168:199-212.

45. Owen, R. L., and Heyworth, M. F. 1985. Lymphocyte migration from Peyer's patches by diapedesis through M cells into the intestinal lumen. In "Microenvironments in the lymphoid system", G. G. B. Klaus, Ed., Plenum Publishing Corp. pp. 647-654.

46. Owen, R. L., and Jones, A. L. 1974. Epithelial cell specialization within human Peyer's patches: an ultrastructural study of intestinal lymphoid follicles. Gastroenterology 66:189-203.

47. Owen, R. L., Pierce, N. F., and Cray, W. C., Jr. 1983. Autoradiographic analysis of M cell uptake and transport of cholera vibrios into follicles of rabbit Peyer's patches. Gastroenterology 84:1267. (Abstr.)

48. Raphael, S. S. 1976. Lynch's medical laboratory technology. 3rd ed. Vol. 2. W. B. Saunders Co., Philadelphia.

49. Reynolds, E. S. 1963. The use of lead citrate at high pH as an electron-opaque stain in electron microscopy. J. Cell Biol. 17:208-212.

50. Robinson, W. F., and Maxie, M. G. 1985. The cardiovascular system. Pp. 201-338. In K. V. F. Jubb, P. C. Kennedy, and N. Palmer. Pathology of Domestic Animals. Vol. 3. 3rd ed. Academic Press, Orlando.

51. Rombout, J. H. W. M., Lamers, C. H. J., Helfrich, M. H., Dekker, A., and Taverne-Thiele, J. J. 1985. Uptake and transport of intact macromolecules in the intestinal epithelium of carp (Cyprinus carpio L.) and the possible immunological implications. Cell Tiss. Res. 239:519-530.

52. Rooney, J. R., II. 1956. Submucosal glands in the bovine colon. Am. J. Vet. Res. 17:599-606.

53. Roy, M. J., Ruiz, A., and Varvayanis, M. 1985. A novel antigen circumscribes groups of lymphoepithelial lymphocytes in gut- and bronchus-associated lymphoid tissues (GALT and BALT). Gastroenterology 88(5):1561.

54. Schmedtje, J. F. 1966. Fine structure of intercellular lymphocyte clusters in the rabbit appendix epithelium. Anat. Rec. 154:417. (Abstr.)

55. Schofield, G. C., and Cahill, R. N. P. 1969. Intestinal and cloacal lymphoepithelial glands in the Australian echidna: a possible homologue of the bursa of Fabricius. J. Anat. 105(3):447-456.

56. Scott, G. B. D. 1982. Mucosal microhernias in the nonhuman primate colon:their role in the pathogenesis of colonic disease. Vet. Pathol. 19(Suppl. 7):134-140.

57. Sheehan, D. C., and Hrapchak, B. B. 1980. Theory and practice of histotechnology. 2nd ed. C. V. Mosby Co., St. Louis, MO.

58. Steel, R. G. D., and Torrie, J. H. 1980. Principles and procedures of statistics: a biometrical approach. 2nd ed. McGraw-Hill Book Co., New York.

59. Tomasi, T. B., Jr. 1983. Mechanisms of immune regulation at mucosal surfaces. Rev. Infect. Dis. 5(Suppl. 4):S784-S791.

60. Torres-Medina, A. 1981. Morphologic characteristics of the epithelial surface of aggregated lymphoid follicles (Peyer's patches) in the small intestine of newborn gnotobiotic calves and pigs. Am. J. Vet. Res. 42(2):232-236.

61. Torres-Medina, A. 1984. Effect of rotavirus and/or Escherichia coli infection on the aggregated lymphoid follicles in the small intestine of neonatal gnotobiotic calves. Am. J. Vet. Res. 45(4):652-660.

62. Van Kruiningen, H. J. 1971. Colitis cystica profunda in animals. Dig. Dis. Sci. 16(4):370-380.

63. Waksman, B. H., and Ozer, H. 1976. Specialized amplification elements in the immune system: the role of nodular lymphoid organs in the mucous membranes. Prog. Allergy 21:1-113.

64. Watanabe, H., Margulis, A. R., and Harter, L. 1983. The occurrence of lymphoid nodules in the colon of adults. J. Clin. Gastroenterol. 5:535-539.

65. Wilders, M. M. 1983. Large mononuclear Ia-positive veiled cells in Peyer's patches II. Localization in rat Peyer's patches. Immunology. 48:461-467.

66. Williams, D. M., and Bertschinger, H. U. 1974. Pathology of the large intestine of piglets with diarrhea and runting. Vet. Pathol. 11:448. (Abstr.)

67. Williams, D. M., and Rowland, A. C. 1972. The palatine tonsils of the pig -- an afferent route to the lymphoid tissue. J. Anat. 113(1):131-137.

68. Wolf, J. L., Kauffman, R. S., Finberg, R., Dambrauskas, R., Fields, B. N., and Trier, J. S. 1983. Determinants of reovirus interaction with the intestinal M cells and absorptive cells of murine intestine. Gastroenterology 85:291-300.

69. Wolf, J. L., Rubin, D. H., Finberg, R., Kauffman, R. S., Sharpe, A. H., Trier, J. S., and Fields, B. N. 1981. Intestinal M cells: a pathway for entry of reovirus into the host. Science 212:471-472.

70. Wolf, J. L., and Bye, W. A. 1984. The membranous epithelial (M) cell and the mucosal immune system. Ann. Rev. Med. 35:95-112.

71. Woode, G. N., Gourley, N. E. K., Pohlenz, J. F., Liebler, E. M., Mathews, S. L., and Hutchinson, M. P. 1985. Serotypes of bovine astrovirus. J. Clin. Microbiol. 22(4):668-670.

72. Woode, G. N., Pohlenz, J. F., Gourley, N. E. K., and Fagerland, J. A. 1984. Astrovirus and Breda virus infections of dome cell epithelium of bovine ileum. J. Clin. Microbiol. 19(5):623-630.

ACKNOWLEDGMENTS

The author is deeply grateful for the support, encouragement, interest, and patience provided and shown by his wife, Karen, and children, Erin, Matthew, and Brian. Without their help the work would not have been completed. They made the effort worthwhile.

My major professor, Dr. Joachim F. Pohlenz, was a constant source of stimulating interest, ever ready to hear and reply to questions of his novice pupil, to interpret findings, and to offer advice. His passion for his work is unmistakable and contagious. It is exciting to share with him a sense of the broader import of the work.

Many individuals have contributed to this work through their technical expertise, generous and valuable advice, or simple moral support. I am indebted to them all, but must especially mention Mrs. Kay Pierce and Ms. Collette Wolter of the histology laboratory and Mss. Jane Fagerland, Sally Pyle, and Sara Mathews of the electron microscopy laboratory. The work was based largely on their technical skill, and their willingness and dedication were deeply appreciated.

Ms. Elisabeth Liebler, because of the similarity of her current studies, and from prior work, was a valued advisor as well as a friend with whom to share both excitement and frustrations.

Prof. Larry Arp, as a good friend, went well beyond duty to share of his time, talents, and knowledge.

Lastly, but far from least, I thank my parents for a whole lifetime of unflagging loyalty, support, and enthusiasm, without which this work would never have begun.

APPENDIX A

Drugs, Reagents, and Formulations

acetone
Acetone, Certified A.C.S.
Fisher Scientific Co., Fair Lawn NJ

acid alcohol, 1%

hydrochloric acid	1.0 ml
Hydrochloric Acid, Reagent A.C.S. Fisher Scientific Co., Fair Lawn NJ	
ethanol, 70%	99.0 ml

cacodylate buffer ($[CH_3]_2AsO_2Na \cdot H_2O$), 0.2M

sodium cacodylate	10.7 g
SPI Supplies West Chester PA	
distilled water (dH_2O)	qv 250.0 ml

epoxy resin

EM bed 812	16.0 g
DDSA (dodecenyl succinic anhydride)	8.0 g
NMA (nadic methyl anhydride)	9.2 g
DMP-30 (2,4,6-tri[dimethylaminomethyl]phenol)	0.3 g

Electron Microscopy Sciences
Fort Washington PA

ethanol, 95%
Chemistry Stores, Iowa State University, Ames IA

ethanol, absolute
Alcohol, Anhydrous, Reagent
J.T. Baker Chemical Co., Phillipsburg NJ

formol sublimate

dH_2O	135.0 ml
$HgCl_2$	8.145 g
formaldehyde, 37%	15.0 ml

Formaldehyde Solution, 37% W/W
Fisher Scientific Co., Fair Lawn NJ

freon
Freon 113 Solvent, Polysciences Inc., Warrington PA

glutaraldehyde, 3%, in 0.1M cacodylate buffer

cacodylate buffer, 0.2M	50.0 ml
glutaraldehyde, 70%	4.3 ml
Purified Glutaraldehyde, 70%	
Ladd Research Industries, Inc., Burlington VT	
dH_2O	45.7 ml
pH adjusted to 7.3	

glutaraldehyde, 3%, and tannic acid, 8% (GTA)
0.08 g tannic acid per ml standard 3% glutaraldehyde in 0.1M cacodylate buffer (see above)
pH adjusted to 7.2-7.3

lead citrate (Reynolds' lead citrate (49))

dH_2O, carbonate-free	30.0 ml
lead nitrate	1.33 g
Lead Nitrate, Certified A.C.S.	
Fisher Scientific Co., Fair Lawn NJ	
sodium citrate•$2H_2O$	1.76 g
Sodium Citrate, Certified	
Fisher Scientific Co., Fair Lawn NJ	
NaOH, 1N	8.0 ml
dH_2O, carbonate-free	qv 50.0 ml

lithium carbonate, saturated

lithium carbonate	1.0 g
Lithium Carbonate, Certified A.C.S.	
Fisher Scientific Co., Fair Lawn NJ	
dH_2O	100.0 ml

methylene blue
Methylene Blue C.I. No. 52015
Fisher Scientific Co., Fair Lawn NJ

Nembutal®, pentobarbital sodium, USP, 50 mg (3/4 gr)/ml
Abbott Laboratories, North Chicago

neutral buffered formalin (NBF; 10% buffered formol saline)

dH_2O	900.0 ml
NaCl	8.5 g
sodium phosphate, monobasic	4.0 g
sodium phosphate, dibasic, anhyd.	6.5 g
formaldehyde, 37%	100.0 ml

Formaldehyde, 37% W/W
Fisher Scientific, Fair Lawn NJ

osmium tetroxide
Osmium Tetroxide, E.M. Grade Purified
Electron Microscopy Sciences, Ft. Washington PA

Permount®, Fisher Scientific Co., Fair Lawn NJ

physiologically buffered saline (PBS)

NaCl	8.5 g
Na_2HPO_4 (anhyd)	1.07 g
$Na_2H_2PO_4 \cdot 2H_2O$	0.39 g
dH_2O	qv 1.0 l

pH adjusted with 1N NaOH to 7.1

sodium borate
Sodium Borate Powder, Fisher Scientific Co., Fair Lawn NJ

tannic acid
Tannic Acid, Certified, Fisher Scientific Co., Fair Lawn NJ

toluidine blue
Toluidine Blue O C.I. 52040, Sigma Chemical Co.
St. Louis MO

uranyl acetate, 2% methanolic

uranyl acetate	0.5 g

Uranyl Acetate, Certified A.C.S.
Ladd Research Industries, Inc., Burlington VT

methanol, absolute	qv 25.0 ml

Methanol, Certified A.C.S.
Fisher Scientific Co., Fair Lawn NJ

xylene
Xylenes, Certified A.C.S., Fisher Scientific Co.
Fair Lawn NJ

APPENDIX B

Use of Individual Animals

Age	Litter[1]	Use
4 wk	Y	histology
9 wk 4 days	O	count
5 wk 3 days	Y	count
10 wk 2 days	O	count
6 wk	Y	SEM, TEM
10 wk 4 days	O	histology, SEM, TEM
11 wk	O	histology (serial sections), TEM
11 wk	O	count
12 wk	O	count
12 wk 1 day	O	TEM
11 wk	Y	histology (serial sections), SEM, nodule "type" survey
12 wk 6 days	Y	histology (serial sections)
13 wk	Y	count
13 wk	Y	count

[1] O = older litter, 31 days older than Y, the younger litter.

APPENDIX C

Pilot Studies

Gross identification of LGCs

In colons fixed by mass infusion with NBF (four pigs) LGCs could not be reliably identified. Rigid tissue folds meant the tissue could not be laid flat; congested areas became an opaque dark brown; submucosal and serosal fat deposits were confused with true LGCs; and LGCs blending with the rest of the intestinal wall were overlooked. Similar difficulties were encountered in an earlier study of human Peyer's patches (15). Neither hydrogen peroxide nor dilute hydrochloric acid were effective in clearing the tissue of the precipitated blood. It was impossible to strip away the serosa in fixed intestine without tearing and fracturing the mucosa and submucosa.

In fixed, uninfused (undistended), and contracted colon LGCs are very difficult to discern, even with transmitted light.

Stripping of the serosa and/or muscular tunics from the mucosa and submucosa of fresh colon (four pigs) was attempted. In two cases it was difficult and substantial tissue damage resulted. Even when accomplished, the mucosa and submucosa were stretched severely, rendering measurement of length and width meaningless. LGCs, at least the larger ones, were clearly seen by transmitted light, however.

Histology and uniformity of lymphoid aggregates

Three preliminary trials were attempted to determine if all grossly observable lymphoid aggregates in colon wall were LGCs or if simple

lymphatic nodules (lacking intimate epithelial association) occurred as well. Ninety-five discrete specimens, collected in more or less random fashion from acetic acid/methylene blue treated colon, uninfused NBF-fixed colon, and NBF infusion fixed colon, were studied. Results of these trials were invalidated by the discovery that substantial amounts of tissue were frequently lost from deep sectioning of blocks, especially if more than one specimen were embedded per block. Nine lymphoid aggregates were totally lost. Extreme caution was indicated for further work (see Table 4). Despite the problems, much information on the basic morphology of the LGC was gained from these specimens.

Preliminary histologic studies of LGCs from five pigs were used to: 1) confirm the distinctiveness of the discrete colonic LGC from peri-ileocecal valve aggregated tissue 2) investigate the value of and establish the methodology for serial sectioning 3) confirm that basic morphological features were preserved despite prolonged washing in water 4) establish that LGCs from older animals (i.e., a 2-year old boar) are similar to those of immature pigs and 5) obtain a sampling of LGCs altered by colonic disease (selected specimens from several other diagnostic cases were also collected).

Electron microscopy

Colons from four pigs were used for pilot studies. Methods of tissue collection included flushing and infusion of whole colons with NBF, infusion of short ligated segments with glutaraldehyde, and immersion fixation of opened specimens in glutaraldehyde; all were collected immediately following euthanasia of the animals.

From these it was learned that: 1) infusion fixation of whole colons often causes overdistention of some portions 2) thorough flushing is essential over surfaces of interest on SEM specimens in order to visualize fine detail (i.e., microvilli) 3) NBF fixed tissues can give reasonable SEM results 4) luminal infusion (gut distention) facilitates localization of LGCs 5) post mortem fixation results in impermissible loss of ultrastructural detail due to autolysis, especially in submucosal regions 6) exudates either obscure surface detail (e.g., microvilli) or confound its interpretation.